Development of analytical tools to enrich and identify protein dopaminylation

Emily J Myers

A dissertation
submitted in partial fulfillment of the
requirements for the degree of

Doctor of Philosophy

University of Washington
2020

Reading Committee:
Shao-En Ong, Chair
Sandra Bajjalieh
Larry Zweifel

Program Authorized to Offer Degree:
Department of Pharmacology

©Copyright 2020

Emily J Myers

University of Washington

Abstract

Development of analytical tools to enrich and identify protein dopaminylation

Emily J Myers

Chair of Supervisory Committee:
Shao-En Ong
Department of Pharmacology

Dopamine homeostasis and oxidative stress are thought to be key players in the etiology of Parkinson's disease (PD). PD is a disorder characterized by the death of dopaminergic neurons in the substantia nigra and the formation of protein aggregates containing α-synuclein. Aberrant cytosolic dopamine levels have been linked to mitochondrial and lysosomal dysfunction, oxidative stress, and increased expression of α-synuclein in dopaminergic neurons. Outside of vesicles, dopamine is rapidly oxidized and accumulates in cells as various polymerized forms including neuromelanin. Oxidized dopamine can also covalently modify nearby proteins leading to structural and functional consequences, including aggregation. Currently, little is known about dopaminylation of proteins as dopamine is not widely recognized as a post translational modification. While several studies have identified dopamine-protein adducts, these studies are limited in scope or rely on *a priori* knowledge of likely candidate proteins due to lack of relevant discovery tools. Here, we describe several non-targeted approaches to investigate dopaminylation, including a method for enrichment, identification, and site-localization of dopaminylated peptides. Our method uses *m*-aminophenylboronic acid resin for covalent capture of the *cis*-diol moiety of dopamine to enrich dopaminylated peptides followed by identification using tandem mass spectrometry. Using this strategy, we identify over 1800 dopaminylated peptides from cultured cells and 20 dopaminylated peptides from post-mortem human brain tissue. In both cultured cells and brain

tissue, we identified dopaminylation at Cys147 in SOD1. SOD1 is a key protein in oxidative stress and neurodegeneration, and modifications of Cys147 promote protein dysfunction and aggregation. We believe these approaches to be powerful tools to characterize site-specific dopaminylation of proteins, enabling mechanistic studies into the role of dopaminylation in the pathogenesis of Parkinson's disease.

List of Figures

List of Tables

Glossary

Abbreviation	Full Name
AADC	Amino acid decarboxylase
ADH	Aldehyde dehydrogenase
ALS	Amyotrophic lateral sclerosis
APLP2	Amyloid-like precursor protein 2
APP	Amyloid precursor protein
ATP	Adenosine triphosphate
ATP13A1	ATPase 13A1
Aβ42	Amyloid-β 42
BAG3	BCL2 associated athanogene 3
BD	Biotin-dopamine
BK	Bromomethyl ketone
BSA	Bovine serum albumin
CAM	Chloroacetamide
CAMK2G	Calcium/Calmodulin dependent protein kinase II gamma
CCB	Colloidal coomassie blue
CDC34	Cell division cycle 34
CISD2	CDGSH iron sulfur domain 2
CNS	Central nervous system
COMT	Catechol-O-methyltransferase
CSF	Cerebral spinal fluid
Cys	Cysteine
DA	Dopamine
DAQ	Dopamine quinone
DASQ	Semiquinone dopamine radical
DAT	Dopamine active transporter
DJ-1	Protein deglycase
DOPAC	3,4-Dihydroxyphenylacetic acid
DOPAL	3,4-Dihydroxyphenylacetaldehyde
DSS	Disuccinimidylsuberate
DTT	Dithiothreitol
DβH	Dopamine-β-hydroxylase
FDR	False discovery rate
GABA	ɣ-Aminobutyric acid
GAPDH	Glyceraldehyde 3-phosphate dehydrogenase
GBA	β-glucocerebrosidase
GPHN	Gephyrin
HCD	Higher-energy collisional dissociation
HEK	Human embryonic kidney

Glossary, cont.

Abbreviation	Full Name
His	Histidine
HMOX2	Heme oxygenase 2
HMW	High molecular weight
HRP	Horseradish peroxidase
HSP	Heat shock protein
HVA	Homovanillic acid
IA	Iodoacetamide
iBAQ	Intensity-based absolute quantification
IMAC	Immobilized metal affinity chromatography
LB	Lewy body
LC	Liquid chromatography
LDAC	Leucodopaminechrome
L-DOPA	Levodopa, l-3,4-dihdroxyphenyalanine
LRRK2	Leucine-rich repeat kinase 2
Lys	Lysine
m/z	Ratio of mass to charge
MAO	Monoamine oxidase
MAPT	Microtubule-associated protein tau
MDMA	Methylenedioxymethamphetamine
MeCN	Acetonitrile
MPTP	1-methyl-4-phenyl-1,2,3,6-tetrahydropyridine
MS	Mass spectrometry
N2A	Neuro-2a, mouse neuroblastoma cell line
NE	Norepinephrine
nIRF	Near-infrared fluorescence
NM	Neuromelanin
PBA	*m*-Aminophenylboronate
PBS	Phosphate buffered saline
PD	Parkinson's disease
PINK1	PTEN induced kinase 1
PPP5C	Protein phosphatase 5 catalytic subunit
PRDX	Peroxiredoxin
PRKN	Parkin RBR E3 ubiquitin protein ligase
PSM	Peptide-spectrum matches
PTM	Post-translational modification
RA	Retinoic acid
ROS	Reactive oxygen species
RTN3	Reticulon 3
SDS-PAGE	Sodium dodecyl sulfate-polyacrylamide gel electrophoresis

Glossary, cont.

Abbreviation	Full Name
SH-SY5Y	Human neuroblastoma cell line
SNCA	α-Synuclein
SNpc	Substantia nigra pars compacta
SOD1	Superoxide dismutase 1
SOD2	Superoxide dismutase 2
TECP	Tris(2-carboxyethyl)phosphine
TFA	Trifluoroacetic acid
TH	Tyrosine hydroxylase
TPA	12-*O*-tetradecanoyl-phorbol-13 acetate
Tyr	Tyrosine
UbE2G1	Ubiquitin conjugating enzyme E2 G1
VMAT2	Vesicular monoamine transporter 2
VTA	Ventral tegmental area
XIC	Extracted ion chromatograms

Acknowledgements

I would like to acknowledge my mentor, Shao-En, for his guidance and support throughout graduate school. The freedom to explore my interests both scientifically and professionally instilled a strong sense of purpose and direction in me. And I am grateful to have learned how to take the failures with the success, and roll with the punches.

I also want to thank my thesis committee members, Sandra Bajjalieh, Larry Zweifel, Ning Zheng, and Jim Bruce who each provided advice and support throughout graduate school. I also want to thank my collaborators who invested in my research by sharing reagents and tissues that were critical to my thesis work: Gary Miller and Dirk Keene. I also want to thank the department of Pharmacology, especially Debbie, Jenny, and Diane.

I acknowledge and thank my lab mates for their guidance, discussion, support, and engagement. Ho-Tak and Martin were instrumental in my training as a scientist, a mass spectrometrist, and a lab community member. I will miss sharing beers on Fridays and cookies any day they were needed.

Next, I would like to thank my cohort: Eedann, Kristine, Rigney, Sabrina, Samara, and Stacey. We started this journey together and I am so grateful for your friendship and for each of your unique perspectives. Eedann, I knew that first of day of recruitment we would be friends and I am so grateful to have your friendship. Rigney, I never imagined a person who is so kind and loving and also an amazing scientist and dancer. I am so proud of you, my sister, and am humbled by your friendship.

I thank my big brother, Samuel Myers, for your support and guidance both throughout graduate school and life. I am unbelievably lucky to have you as a role model, colleague, and friend. Sam, you may not have been on my thesis advisory committee, but you will always be on my life advisory committee.

I also thank my mother Jill for always encouraging me to follow my dreams and create a life filled with love. To my grandfather Don, who nurtured my curiosity about the word and answered my unending questions, thank you. I know you will always walk beside me. And to my dearest friend Kim, thank you for your love and for always being my home base.

Finally, I thank my women scientist friends: Sarah Myhre, Jeanna Wheeler, Heather Currey, Laura Osburn, Jodie Katon, Katie Reichard, and Sharona Gordon. With each of you, I have found community and nourishment throughout my time in graduate school and am thrilled to support you on your journeys ahead.

1.1. Dopamine and its Role in Physiology

Dopamine (DA) is one of the most important and abundant catecholamines in the human body. DA is a common precursor to other neurotransmitters including epinephrine and norepinephrine and is itself a critical neurotransmitter. In the periphery, DA acts as an important hormone for electrolyte balance and is a primary neurotransmitter in important functions such as reward, cognition, movement and motor control, and lactation. Therefore, disruption of DA homeostasis and signaling can lead to disease and psychiatric disorders such as Parkinson's Disease, schizophrenia, and substance abuse disorders [1, 2]. In humans, DA is synthesized via the conversion of phenylalanine to tyrosine by phenylalanine hydroxylase, catalyzing the addition of the hydroxyl group to the benzene ring. Next, a second hydroxyl group is added to the benzene ring by tyrosine hydroxylase (TH) to form levodopa (L-DOPA); this is the rate-limiting step (Scheme 1.1). L-DOPA is then converted to DA by amino acid decarboxylase (AADC). DA may be processed further by dopamine-β-hydroxylase (DβH) to form norepinephrine and by phenylethanolamine-N-methyltransferase to form epinephrine [3].

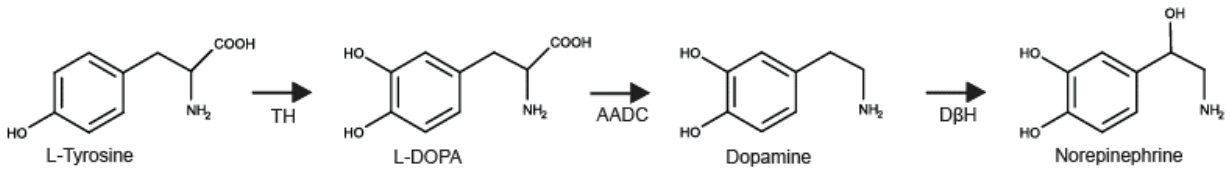

Scheme 1.1: **Biosynthesis of dopamine** from tyrosine hydroxylase (TH) and amino acid decarboxylase (AADC). Dopamine can be converted to Norepinephrine by Dopamine-β-Hydroxylase (DβH).

After synthesis, catecholamines are packaged into vesicles by vesicular monoamine transporter 2 (VMAT2) to be stabilized and transported to the axon terminal. In dopaminergic (DAergic) neurons, the vast majority of DA is stored in synaptic vesicles with an internal acidic pH of about five, hindering DA from rapid autoxidation which occurs at physiological pH ~7.4 [4]. Some studies have suggested that enzymes of DA synthesis, TH and AADC, physically associate with VMAT2 to prevent DA in the cytosol

[5]. In DAergic neurons, like most neurons, chemical neurotransmission is initiated by a depolarization of the presynaptic terminal often due to an action potential. Upon depolarization, synaptic vesicles fuse with the plasma membrane, releasing DA into the synaptic cleft where it can interact with DA receptors.

DA receptors are G-protein coupled receptors prominent in the central nervous system, cardio-pulmonary system, and renal system. DA receptors can be divided into two general subtypes: G_s coupled (D1 and D5) and G_i coupled (D2, D3, and D4) to affect downstream signaling [6]. Neurotransmission is halted when DA is cleared from the synapse, through both diffusion and uptake by the dopamine transporter (DAT) and recycled or degraded (Figure 1.1). The major metabolic pathway for DA degradation starts with monoamine oxidase (MAO) acting on DA through oxidative deamidation to produce 3,4-dihydroxyphenylacetaldehyde (DOPAL), hydrogen peroxide, and ammonia. DOPAL is converted to its acid (DOPAC) by aldehyde dehydrogenase (ADH). DOPAL and DOPAC metabolites are also easily oxidized [7]. Finally catechol-O-methyltransferase (COMT) converts DOPAC to the nonreactive metabolite homovanillic acid (HVA) [8].

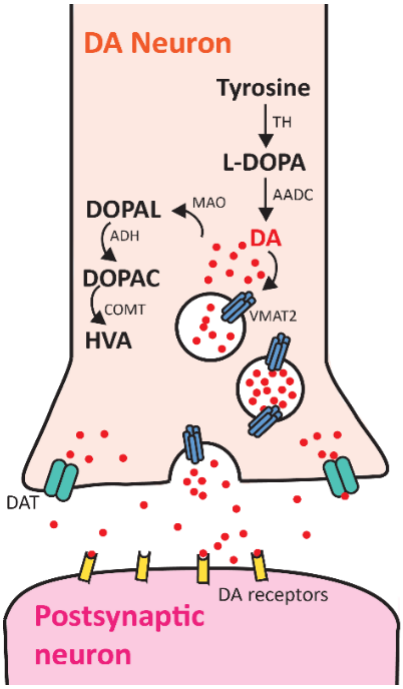

Figure 1.1. Dopamine metabolism in the neuron. As L-DOPA is converted to DA by AADC, DA is transported into synaptic vesicles by VMAT2. Unpackaged DA in the cytosol undergoes oxidative deamidation by MAO to produce DOPAL, which undergoes additional reactions to produce unreactive HVA. When stimulated, the neuron releases DA into the synaptic cleft to transduce signal to post-synaptic DA receptors. Excess DA is transported back into the presynaptic neuron via DAT and either recycled or degraded.

The DA molecule appears simple: a primary amine connected by an ethyl chain to a benzene ring with two hydroxyl groups (a catechol), but DA's chemistry is complex. DA, and to a lesser extent other catecholamines, are spontaneously oxidized to form dopamine quinone (DAQ) in the presence of ambient oxygen, reactive oxygen species, redox-capable metals, peroxidases, and at neutral pH [9]. DAQ is capable of many downstream reactions including protein modification (dopaminylation) and forming DA polymers. Some plants and animals use these reactions to their advantage. For example, zebra mussels incorporate DA into their foot proteins where DA forms protein aggregates and covalent attachments with rocks upon exposure to the basic ocean water at pH 8.1 [10, 11]. Grasshoppers use polyDA to crosslink the structural proteins in the mandible to strengthen the mandible and prevent breakdown [12]. Simply stated, dopamine can be used as a glue to crosslink proteins together and form insoluble aggregates. In the brain, insoluble protein aggregates are toxic and the bases for several neurodegenerative diseases. Therefore, to protect against potential "protein glue", DA must be tightly regulated and contained. If DA leaks into the cytosol, DA will oxidize at cytosolic pH and may modify nearby proteins. Small amounts of dopaminylation is unlikely to induce cell death, but cells may accumulate modified proteins as they age, eventually leading to protein aggregates. While protein aggregation is a common feature in many neurodegenerative diseases, the role of dopamine modifications in protein aggregation remains unknown. Tools to study DA as a protein post-translational modification (PTM) are limited, and currently no unbiased method exists to identify specific protein sites of dopaminylation.

1.2. Neural Circuitry of Dopamine Pathways

Identification of DA as a neurotransmitter in the brain was a key finding by Arvid Carlsson and led Carlsson, Eric Kandel, and Paul Greengard to win the Nobel Prize in Physiology or Medicine in 2000 for their work on catecholamine neurotransmission [13]. Since their discovery four major DA circuits have been described in the brain: mesocortical, mesolimbic, nigrostriatal, and tuberoinfundibular pathways. The tuberoinfundibular pathway DAergic neurons project from the arcuate nucleus of the hypothalamus to the pituitary gland to affect prolactin release. In the mesocortical pathway, DAergic neurons project from the ventral tegmental area (VTA) to the prefrontal cortex and are implicated in cognitive and emotional behavior. The mesolimbic pathway also originates with DAergic neurons in the VTA and projects to

multiple areas of the limbic system, including the olfactory bulb, amygdala, piriform cortex, lateral septal nuclei, and the nucleus accumbens. In this neural circuit, DA functions in emotion and reward systems. [14] Together, the mesolimbic and mesocortical dopamine circuitry are engaged in reward learning and concentration, whereas dysfunction in this circuitry contributes to neuropsychiatric disorders including substance abuse disorder, attention deficit disorders, and schizophrenia [15].

The DAergic neurons of the nigrostriatal pathway have cell bodies in the substantia nigra pars compacta (SNpc) and project to the caudate nucleus and the putamen in the striatum. The release of DA in the striatum plays a significant role in motor function, regulating the direct and indirect pathways important for fine motor control. In collaboration with other neurotransmitters like glutamate and γ-aminobutyric acid (GABA), DA activation of D1-like receptors of the putamen, the “direct” pathway, activates the motor cortices, while DA activation of D2-like receptors reduces activation of motor cortices, stymieing voluntary movement [16]. Disruption of this system leads to loss of fine motor control and difficulties initiating movement, and the loss of DAergic neurons in the SNpc produce the classical symptoms of Parkinson’s disease: akinesia, rigidity, and tremor at rest.

Altered DA homeostasis in the central nervous system (CNS) is implicated in many other psychiatric and neurodegenerative disorders beyond Parkinson’s disease. Schizophrenia is associated with increased amphetamine-stimulated striatal DA release. DA pathway dysfunction has been implicated in other mood disorders like depression and mania [17]. Many addictive drugs act on the dopamine system, and pharmacological blockade of DA signaling can attenuate drug-associated reward [18]. DA neurotransmission has also been implicated in Alzheimer’s disease, Huntington’s disease, and multiple sclerosis, among others [19].

1.3. Parkinson’s Disease

Parkinson’s disease affects an estimated 10 million people worldwide and is the second most common neurodegenerative disorder. This debilitating movement disorder is a result of degeneration of several neuronal populations, however, SNpc DAergic neurons are impacted early, leading to loss of DA in the nigrostriatal system. Death of these neurons is progressive and early intervention is difficult as

onset of clinical motor symptoms are associated with loss of 70-80% of striatal DA. PD can be classified into four sub-types: 1. Idiopathic Parkinson's (or Primary Parkinson's) disease where the underlying mechanisms are unclear; 2. Acquired Parkinson's (or Secondary) disease which stems from exposure to toxins; 3. Hereditary Parkinson's disease which has a direct, genetic basis, and 4. Parkinson's-like or Parkinson's-plus syndromes which represents a larger variety of diseases with similar symptoms and pathology, including Dementia with Lewy Body disease and related synucleinopathies [20]. The canonical symptoms of PD include tremor, dyskinesia and slow movement, rigidity, and progressive motor dysfunction. Motor dysfunction is the main symptom at time of diagnosis, non-motor symptoms develop much earlier but are often go undiagnosed. These include altered circadian rhythm, hyposmia, depression, speech impairments, and constipation [21]. As disease progresses, additional non-motor symptoms manifest including pain, fatigue, cognitive impairment, orthostatic hypotension, and dementia [22].

The etiology of Parkinson's disease is still largely unknown, although age, sex, genetics, and environmental exposures have all been implicated. The majority of cases of PD (up to 90%) are considered sporadic and have no direct genetic cause [23]. However, improvements in genome sequencing technology have allowed researchers to identify a number of genes that are implicated in disease, including *SNCA, PRKN, PINK1, DJ-1, LRRK2, GBA,* and *MAPT* [24]. Several of the proteins from these genes are known to be prion-like and prone to aggregation. Specifically, α-synuclein *(SNCA)* aggregates to form insoluble fibrils and are the major component in Lewy bodies [25]. Tau, when hyperphosphorylated, self-assembles in "tau tangles" to form insoluble plaques. In addition to prion-like proteins, transition metals with redox activity have also been implicated in the development of protein aggregates in PD [26]. Patients with PD have higher levels of iron in the substantia nigra compared to controls and copper levels are known to be elevated in the cerebral spinal fluid (CSF) of PD patients [27, 28]. Exposure to these metals promote oxidative stress and catalyze oligomerization of α-synuclein in the brain [28, 29]. Other toxins including pesticides and herbicides are thought to play a role in disease through increasing oxidative stress [30]. Rotenone, paraquat, dichlorodiphenyltrichloroethane (DDT), dichlorophenoxyacetic acid, diazinon, chlorpyrifos, propargite, dieldrin, benomyl, maneb, and arsenic

exposure have been directly correlated to increased risk of PD [31]. Due to the multifactorial nature of this disease, it is likely an interaction of genetics and environmental factors that lead to most cases of PD.

The role of dopamine in PD

The selective loss of DAergic cells in PD begs the question of both if and how DA contributes to disease progression. Without tight regulation, DA is toxic *in vivo* and autoxidizes to form to reactive DA metabolites, producing reactive oxygen species (ROS) including O_2^- and H_2O_2 [32]. Due to the clear toxic effects of DA, DA metabolism and storage is an active area of research for neurobiologists. Studies in post-mortem brain tissue suggest Parkinson's patients have lower expression of mRNA for both *DAT* and *VMAT2* per cell and significant loss of VMAT2 function [33, 34]. Decreased expression and pharmacological inhibition of VMAT2 result in Parkinson's-like symptoms and neurodegeneration in animal models [35]. Recently, mutations in *VMAT2* that reduce function were linked to an infantile parkinsonism-like condition [36]. Conversely, increased expression of *VMAT2* has been associated with decreased risk of PD and improved outcomes for DA toxicity [35]. Decades of research demonstrate the importance of strict control and modulation of DA, however, the full consequence of mismanaged DA and its toxicity remains to be seen.

1.4. Dopamine Reactivity and Chemistry

DA is widely acknowledged as toxic, both *in vivo* and *in vitro*. The relatively low free energy barrier to oxidation of DA means it is a highly reactive molecule and can undergo spontaneous autoxidation. Reactivity of DA increases under certain conditions, such as higher pH and the presence of redox-active metals or other oxidants like oxygen or H_2O_2 [37]. DA reactions are complex and can proceed through one or two electron processes to generate semiquinone dopamine radical (DASQ) or dopamine quinone (DAQ), respectively. These reactive intermediates can undergo further oxidation or spontaneous rearrangement to generate other reactive species which can modify proteins, oligomerize to form polydopamine chains and neuromelanin (NM), react with antioxidants like ascorbate and glutathione, or some combination of these depending on reaction conditions [32]. (Scheme 1.2)

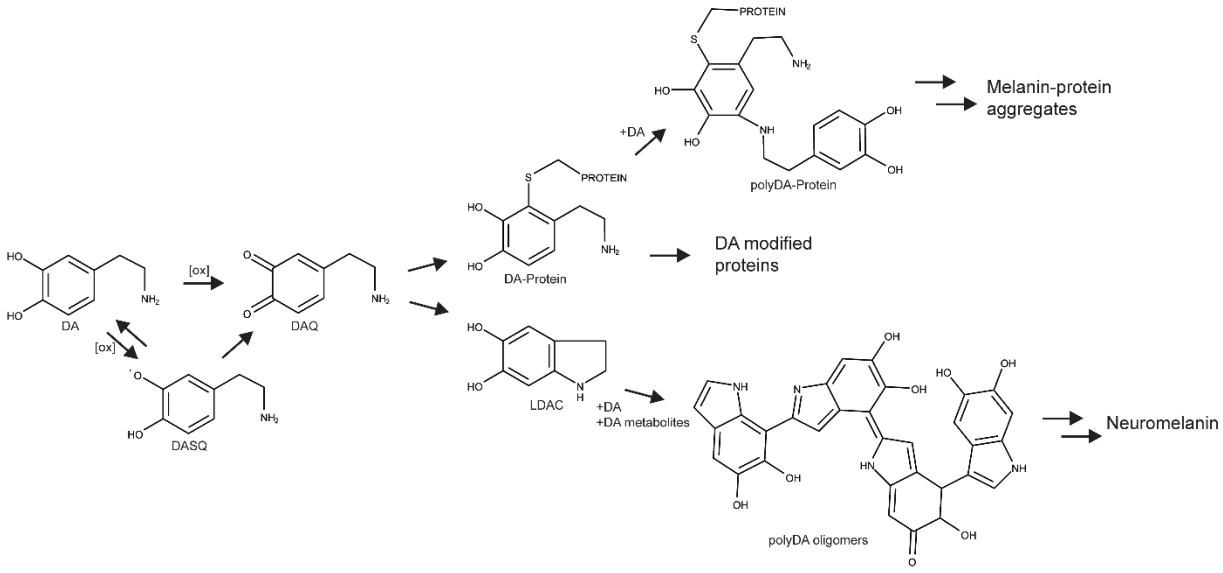

Scheme 1.2: **Steps of DA oxidation to form neuromelanin** from DAQ by DA oxidative polymerization (bottom). DAQ also modifies cysteine side chains (middle) and can form poly-dopamine cysteine conjugates (top).

In vivo, DA oxidation can be induced via H_2O_2 activation by heme or peroxidases, prostaglandin H synthase, and activated microglia [38-40]. The presence of redox-active metal ions, such as copper and iron, have also been implicated in DA induced neurodegeneration. For example, iron accumulates in Lewy bodies of PD patients, and plaque deposits in Alzheimer's patients contain iron bound by amyloid-Beta [41, 42]. Researchers have also shown both copper and iron are necessary for the aggregation of α-synuclein and elevation of DA levels induces aggregation [43]. DA oxidation promoted by metal ions can generate several toxic species including DAQ, DASQ, $O_2^{\cdot-}$, H_2O_2, and $^{\cdot}OH$, creating a cascade of ROS and oxidative stress [9].

Neuromelanin

Neuromelanin is a dark pigment found primarily in DAergic neurons of the SNpc and noradrenergic cells of the locus coeruleus. NM is formed from the polymerization of DA and other catecholamines (Scheme 1.2) and is structurally similar to other melanins, such as melanin found in skin. The precursors to NM and melanin overlap: tyrosine, L-Dopa, DA, norepinephrine, and thiols [44]. However, unlike melanin synthesis which is tightly controlled through enzymatic reactions, generation of

NM appears to be non-enzymatic and driven by autoxidation of catecholamines to quinones, polymerization of quinone species, and recent studies suggest a role for cytosolic seeds of aggregated protein or peptides in NM formation [45-47]. pH is also critical to DA oxidation as at physiological pH or higher, the protons of the hydroxyl groups dissociate to form an electrophilic quinone, whereas DA at the vesicular pH (pH ~5) is stable [4]. Redox-active metals likely play a role in NM catalysis; NM isolated from the SNpc also contains significant amounts of metal ions, especially iron [48]. The resulting chemically complex NM precursors, a mixture of DA and its derivatives, proteins, and metal ions, are engulfed in autophagic vacuoles and fuse with lysosomes for degradation. However, lysosomal proteases are unable to degrade NM precursors [47]. As the autolysosome fuses with other lysosomes and autophagic vacuoles, NM precursors continue to accrue modifications including different proteins and lipids from other lysosomes [47, 49]. Eventually, the NM complex is sequestered into specialized double membrane autolysosome where it accumulates.

Human and primate brains have higher levels of NM compared to other vertebrates, and small vertebrates like mice have almost undetectable levels making NM difficult to study in animal models [50, 51]. In humans, dark, pigmented cells are absent at birth, but NM can be seen by age 5 and continues to accumulate throughout a lifetime [52]. This complex molecule has been used as a hallmark for Parkinson's disease and implicated in other age-related neurodegenerative diseases. The loss of pigmentation in the SNpc, where NM-rich cells undergo cell death unlike non-pigmented DAergic cells in the VTA, is a classic characteristic of Parkinson's disease. However, the formation of NM may provide a protective mechanism against accumulation of cytosolic DA by binding quinones and buffering against subsequent ROS [53]. NM may act to chelate and trap metals, bind proteins including ferritin, and sequester neurotoxins like paraquat and 1-methyl-4-phenyl-1,2,3,6-tetrahydropyridine (MPTP) [54-56]. It is proposed that as NM accumulates these toxins, metals, and modified proteins, its capacity diminishes and these are released back into the neuron, resulting in cell death [55, 57, 58] Once freed from the granule, NM itself can activate microglia, initiate an inflammatory response, and exacerbate damage to surviving cells [59]. While NM is thought to play a protective role in DAergic neurons, the accumulation of toxins may contribute to age-related neuron loss. A complete picture of the function and structure of NM and its role in PD has not been fully elucidated at this time.

Protein modification by DA and its derivatives

The modifications of proteins by DA and its oxidation products have long been thought to be a major component of DA toxicity. The autoxidation of DA under physiological pH leads to DAQ formation, a strong electrophile, and generates ROS. Studies from the 1980s demonstrated DA's toxic reactivity towards nucleophilic protein side-chains, specifically Cys, His, and Lys residues [60, 61]. *In vitro* studies with free amino acids or small peptides found that the thiol groups of Cys residues were highly susceptible to DA modification; Cys modification is preferred over ring closure to form leucodopaminechrome (LDAC) (shown in Scheme 1.2) [62]. Research in this field is ongoing and relies heavily on candidate-driven approaches and *a priori* knowledge of cellular stress. For example, in isolated mitochondria exposed to DA, proteins of complex I, III, and IV of the mitochondrial electron transport chain were found to be dopaminylated and showed reduced ATP production [63]. Actin, tubulin, GAPDH, parkin, GBA, SOD2, and other cysteine containing proteins have also been described as dopaminylated [63-65]. Furthermore, DA metabolites like DOPAL, have also been shown to modify both thiol and amine groups in proteins [66, 67]. DA and DOPAL mediate the aggregation of α-synuclein, the primary component of Lewy bodies, and DOPAL modified α-synuclein can activate microglia [68]. It is clear that accumulation of DA and reactive metabolites depletes cellular stores of antioxidants and increases ROS, promotes protein aggregation and modifications that lead to apoptosis, and increase microglia activation and inflammation in the brain. Unfortunately, technologies previously available to study dopaminylation have been very limited and currently there are no unbiased methods to identify dopaminylated sites on proteins from biological samples. Much of the previous work used purified proteins and DA oxidation, which is unlikely to accurately predict dopaminylation in cells. One previous study relied on treating mitochondria with radiolabeled DA and 2-D gels coupled to LC-MS/MS to nominate potentially dopaminylated proteins. However, without identification of specific sites of DA modification (site IDs), functional analysis of dopaminylation is remained elusive. A more comprehensive methodology is needed to identify modification sites on individual proteins from *in vivo* DA breakdown, to understand how DA modifications affect protein structure and function, and to identify localization of toxic DA reactions in cells. Furthermore, an unbiased approach to identify protein dopaminylation from biological samples

would be clinically relevant as none of the current methods can be applied to identify dopaminylation in human post-mortem brain tissue.

1.5. Mass Spectrometry to Study Post-Translational Modifications

Post-translational modifications (PTMs) multiply the complexity of the proteome beyond the genetically encoded protein sequence. PTMs covalently modify amino acid side chains and increase the variety of functional groups beyond the standard 20 amino acids. These modifications include phosphorylation, glycosylation, acetylation, ubiquitination, etc. and can affect a protein's function, localization, stability, or interaction partners. Proteins have a variety of possible PTMs and the addition/removal of PTMs are commonly used in cellular signaling cascades. Many PTMs are added enzymatically, but non-enzymatic PTMs also exist. For example, advanced glycation end products are a collection of modifications on lysines and arginines that are associated with metabolic stress from glucose metabolism. In high glucose conditions, the degradation of reducing sugars produces reactive species that modify proteins [69]. These modifications have been associated with serious health conditions, including the development of atherosclerotic plaques as well as uncontrolled blood sugar levels in diabetes mellitus.

PTMs can be detected and identified by a variety of methods. Antibody-based methods, in which an antibody is raised against a PTM side chain, are used to detect PTMs via Western blot and immunofluorescence. Such antibodies that recognize specific PTMs have also been important in studying the functional importance of these PTMs in certain biological contexts, examples include phosphotyrosine-specific antibodies (4G10) or antibodies against epigenetic marks like Histone H3 lysine 9 tri-methylation (H3K9me3) [70, 71].

Alternatively, proteomic approaches to study PTMs utilize mass spectrometry (MS). MS is a powerful and unbiased analytical technique that identifies proteins or peptides, including their modified forms, by measuring their mass to charge (m/z) ratio of precursor ions and subsequent product ions to determine peptide sequence. To do this, proteins are extracted from biological samples and digested to peptides. Peptides are then separated via liquid chromatography (LC) over time, introduced into the gas

phase by electrospray ionization, and injected into a MS. The MS measures the m/z values for ions, fragments them and analyzes mass of these fragments to produce a tandem mass spectrum (MS/MS). On state-of-the-art MS instrumentation, a single LC-MS/MS run may produce tens of thousands of mass spectra for complex peptide samples. Mass spectra are analyzed using automated peptide identification software like MaxQuant/Andromeda, which searches the MS spectra against the user specified library of possible peptides [72]. To identify PTMs, we expand our searches to include mass shifts of the modification of interest.

For PTM analysis, it is often necessary to enrich pools of modified proteins or peptides from the bulk protein sample as PTMs are substoichiometric, typically representing a small fraction of total protein present in the cell. MS is typically used to analyze modified proteins or peptides isolated with affinity or covalent capture enrichment from complex mixtures. One of the most widely used affinity-MS methods is immobilized metal affinity chromatography (IMAC) enrichment of phosphorylated peptides coupled with LC-MS/MS. This method has expanded our understanding of the phosphoproteome exponentially by allowing researchers to study how phosphorylation patterns differ in cell types and change in cell signaling and disease states. Unlike phosphorylation, however, enrichment strategies for DA-modified peptides and proteins have not been explored for unbiased proteomics in such depth. This work addresses strategies to enrich and identify dopaminylation with LC-MS/MS.

2.1. Introduction

PD affects an estimated 10 million people worldwide and is the second most common neurodegenerative disorder. This movement disorder is a result of degeneration of several neuronal populations, however, substantia nigra pars compacta dopaminergic neurons are impacted early, leading to loss of DA in the nigrostriatal system [20]. Death of these neurons is progressive and takes years as onset of clinical motor symptoms are associated with loss of 70-80% of striatal DA. In addition to neurodegeneration, DA metabolism and resulting oxidants have been implicated in synaptic nerve terminals damage caused by psychoactive drug use, including cocaine, methamphetamine, and methylenedioxymethamphetamine (MDMA) [73-75]. Furthermore, known environmental toxins such as 1-methyl-4-phenyl-1,2,3,6-tetrahydropyridine (MPTP) and rotenone cause oxidative damage to dopaminergic neurons, which may be exacerbated by excess DA metabolism and altered DA homeostasis [76, 77].

The toxic effects of DA are thought to be attributed, in part, to increases in cytosolic DA, which is rapidly oxidized at physiological pH and modifies proteins and peptides (7). Protein dopaminylation can alter function and structure of proteins and is an important outcome of increases in cytosolic DA. However, dopaminylation is relatively unrecognized as a PTM despite its implications in PD. Currently, studies of dopaminylation are limited to a few proteins due to lack of unbiased tools to identify dopaminylated proteins. For example, proteins which have been identified as dopaminylated were treated to high doses of DA on purified proteins [64, 65]. These studies fail to provide direct evidence of dopaminylation in physiologically relevant conditions. Other groups have used ^{14}C-DA to treat isolated mitochondria or cell lines to indirectly identify several dopaminylated proteins, but this assay does not specify dopaminylation at specific sites [63, 78]. Furthermore, neither of these approaches can be translated to a wide range of biological and/or clinical samples. Most importantly, these techniques cannot be used in clinical investigations to validate targets of dopaminylation or further elucidate functional consequences as they rely on radioactive labeling or purified candidate proteins. Common approaches to

study PTMs, including antibodies to dopaminylation or affinity enrichment coupled to LC-MS/MS, have yet to be developed. Therefore, compared to other PTMs, dopaminylation remains relatively under-examined.

This work will describe a novel chemical biological method for enrichment and identification of native dopaminylated peptides extracted from cells or tissues via mass spectrometric-based proteomics. We a use boronic acid-based covalent capture strategy, commonly used for enrichment of peptides bearing other PTMs such as glycosylation and PARylation, for DA-modified peptide enrichment [79, 80]. This matrix, *m*-aminophenylboronate acid agarose (PBA), covalently but reversibly binds molecules bearing *cis*-diols groups by forming boronic esters. We take advantage of the *cis*-diol moiety of dopamine to capture dopaminylated peptides on PBA beads, release these peptides by hydrolysis in acidic conditions, and analyze peptides via LC-MS/MS. We demonstrate enrichment of thousands of dopaminylated peptides from 2 mg of protein with ~90% of total peptide signal from dopaminylated peptides. We also identify dopaminylation sites on several key proteins implicated in oxidative stress and DA metabolism. This method may facilitate future studies to identify pathological events leading to dopaminergic neuron death in neurodegenerative conditions such as PD.

2.2. Results

2.2.1. Dopamine modifies proteins *in vitro*

Since DA reactivity is highly variable and can result in polyDA chains, melanin, and single or multiple protein modifications including crosslinks, we initially sought to establish experimental conditions to quickly induce single protein modifications and avoid extensive crosslinks and complicated polyDA species. We tested various concentrations of DA on several different purified proteins: Aβ42, CDC34 and UbE2G1. Aβ is of interest due to its established role in neurodegeneration and propensity to aggregate. Alternatively, CDC34 and UbE2G1 were chosen due to their availability. Unfortunately, both Aβ42 and CDC34 are prone to spontaneously form higher molecular weight species even in the absence of DA (data not shown). Further experiments used UbE2G1 as it does not self-aggregate and contains residues predicted to be modified by DA (Fig 2.1A). Multimeriziation of UbE2G1 was seen with treatment with 100 μM of pre-oxidized DA (designated with an *), 100 μM, and 10 μM of DA, showing dimers, trimers, and higher by SDS-PAGE due to DA's ability to form intermolecular protein crosslinks [81]. Additionally, there

appears to be a lower molecular weight band which is indicative of intramolecular crosslinks, as shown by our disuccinimidylsuberate (DSS) control (Figure 2.1B)

After confirming DA's ability to modify and crosslink UbE2G1, we looked to shorten our 96 hour incubation time to decrease degradation products and increase experimental efficiency. To decrease reaction time, we hypothesized that a peroxidase could be used to increase the reaction kinetics. Peroxidases, like horseradish peroxidase (HRP), are known to catalyze DA oxidation in the presence of H_2O_2 [39]. Therefore, we used a combination of IgG-HRP, DA, and H_2O_2 to treat UbE2G1 for 25 min. This reaction yields high molecular weight (HMW) products, some which appear too large to enter the gel (Figure 2.1C). HRP controls were included to distinguish UbE2G1 from IgG-HRP and any unintended cross-linked species. UbE2G1 crosslinks are seen in 25 minutes in the presence of DA without HRP (Figure 2.1C, lanes 5 & 6). However, in the presence of HRP, there was an increase in higher molecular weight species (lanes 2 & 4). Activation of HRP with H_2O_2 generates increased high molecular weight (HMW) species and depletion of monomers of UbE2G1 at 20 kDa (lane 1 & 3). In addition to these HMW species, HRP catalyzed oxidation of DA generated black pigments in the test tube (not shown), consistent with oxidative products polymerizing, including polyDA and melanin (see Scheme 1.2 for details). Peroxidase activity increased kinetics of the reaction, but the high concentration of DA and rapid oxidation induced aggregation that are challenging for downstream mass spectrometry analysis.

To address these challenges, we tested our peroxidase-catalyzed reaction with variable concentrations of DA. In the presence of IgG-HRP, H_2O_2, and 100 μM, 10 μM, or 1 μM DA, similar amounts of intermolecular cross-linked proteins are seen across DA concentrations. To determine which concentration of DA generated protein modifications without crosslinks, we used near-infrared (nIRF) imaging to detect the quinone group of the dopaminylated protein [82]. Interestingly, 10 μM DA shows a 5-fold increase in quinone fluorescence compared to the 100 μM DA (Figure 2.1.D-E). Despite our visualization of dopaminylated proteins, when we excised the fluorescent gel band, digested, and ran LC-MS/MS, we were unable to detect dopaminylated peptides.

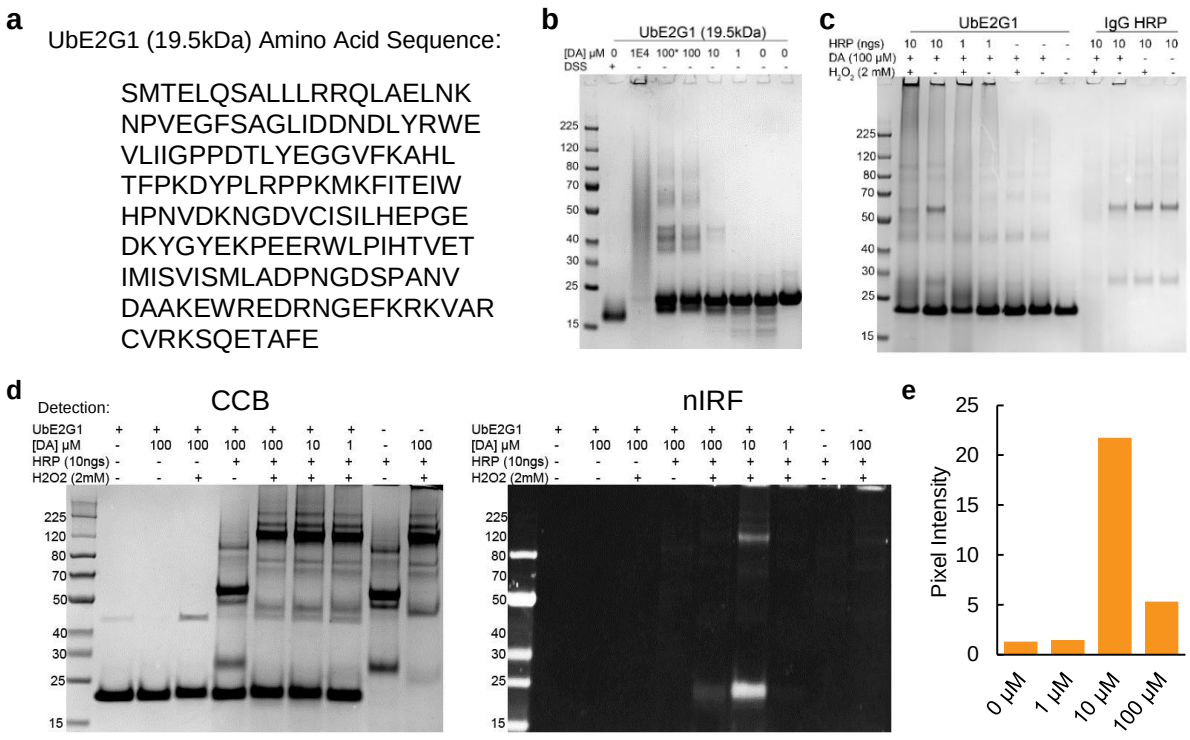

Figure 2.1. Dopamine oxidation and protein modification a) UbE2G1 amino acid sequence which contains potential residues of interest: C, H, K, Y. **b)** UbE2G1 (5 µg) was incubated with 10 mM, 100 µM pre-oxidized*, 100 µM, 10 µM, or 1 µM DA for 96 hours and analyzed by SDS-PAGE stained with Colloidal Coomassie Blue (CCB) to visualize protein. **c)** UbE2G1 (5 µg) was incubated with 100 µM DA, 2 mM H_2O_2, and IgG-HRP for 25 minutes and analyzed by SDS-PAGE stained with Colloidal Coomassie to visualize protein. Lanes with IgG-HRP are run as controls. **d)** UbE2G1 (5 µg) was incubated with HRP, H_2O_2, and 100 µM, 10 µM, or 1 µM DA for 25 minutes and analyzed by SDS-PAGE. Gels were scanned using a near-infrared imager (right panel), then stained with Colloidal Coomassie Blue (CCB) to visualize total protein (left panel). **e)** The fluorescent signal was quantified by measuring pixel intensity at 20kDa and dividing by background pixel intensity. The molecular weight marker on the left side of the gel indicates protein size in kDa. DA=Dopamine, DSS= disuccinimidyl suberate

2.2.2. Enrichment of dopaminylated peptides and site localization

Excess cytosolic DAis a known source of oxidative stress in the brain through formation of DAQ and other toxic metabolites [9]. Formation of DA oxidation products drive DA oxidative polymerization (neuromelanin) and aberrant protein modification through Michael addition with nucleophilic residues Cys, His, and Lys [60, 83]. Tyrosine should also be considered for dopaminylation as Tyr are the primary residue of modification in other peroxidase-catalyzed protein modification [84].

To identify potential sites of dopaminylation, we incubated synthetic peptides containing our residues of interest: Cys, His, Lys, and Tyr with DA (Table 2.1). We first sought to replicate our ability to modify proteins and tested peptide dopaminylation under either ambient oxygen or oxidizing conditions (HRP and H_2O_2). After the reaction, peptides were then desalted and subjected to LC-MS/MS to identify dopaminylated residues. We identified single DA modifications on peptides containing cysteine, but were unable to detect dopaminylation of other residues. An example MS/MS spectra from a dopaminylated synthetic peptide is shown in Fig 2.2A.

Table 2.1: Synthetic peptides

Peptide Sequence	Residue Target	Monoisotopic Mass M+H	Predicted Monoisotopic Mass DA-M+H	Detected as Modified
ADSGEGDFLAEGGGVR	Control	1536.6925	1687.7558	No
LPASFDAR	Control	876.4574	1027.5207	No
EIAQDFKTDLR	K	1335.6903	1486.7536	No
FKRIVQRIKDFLRNLV	K	2045.2495	2196.3128	No
LVEALYLVSGERG	Y	1405.7686	1556.8319	No
LLIYWASTR	Y	1122.6306	1273.6939	No
HTGREIVDLMCHAT	C, H	1582.7465	1733.8098	Yes
KPVAFSDYIHPVCLPDR	K, Y, C, H	1957.0000	2108.0633	Yes

To devise a strategy to enrich for DA-modified peptides, we hypothesized that dopaminylated peptides can be covalently captured by PBA-agarose via DA's *cis*-diol moiety (Fig 2.2B). Boronic-acid based affinity enrichment has been utilized in tandem with LC-MS/MS to study ADP-ribosylation and glycosylation of proteins and peptides [79, 80]. To test this hypothesis, we used PBA to selectively enrich dopaminylated peptides from a pool of unmodified peptides and used LC-MS/MS to quantify each peptide species. We compared peak areas from extracted ion chromatograms (XICs) of dopaminylated-peptide to unmodified peptide before and after enrichment and found a 2.5-fold increase in dopaminylated peptide signal after PBA enrichment (Fig 2.2C). Aiming to maximize the ratio of DA-peptide to unmodified peptide,

we optimized our protocol through several iterations until we saw high specificity for dopaminylated peptides (Fig 2.2D). These results suggested PBA agarose can be used to specifically enrich dopaminylated peptides for identification by LC-MS/MS.

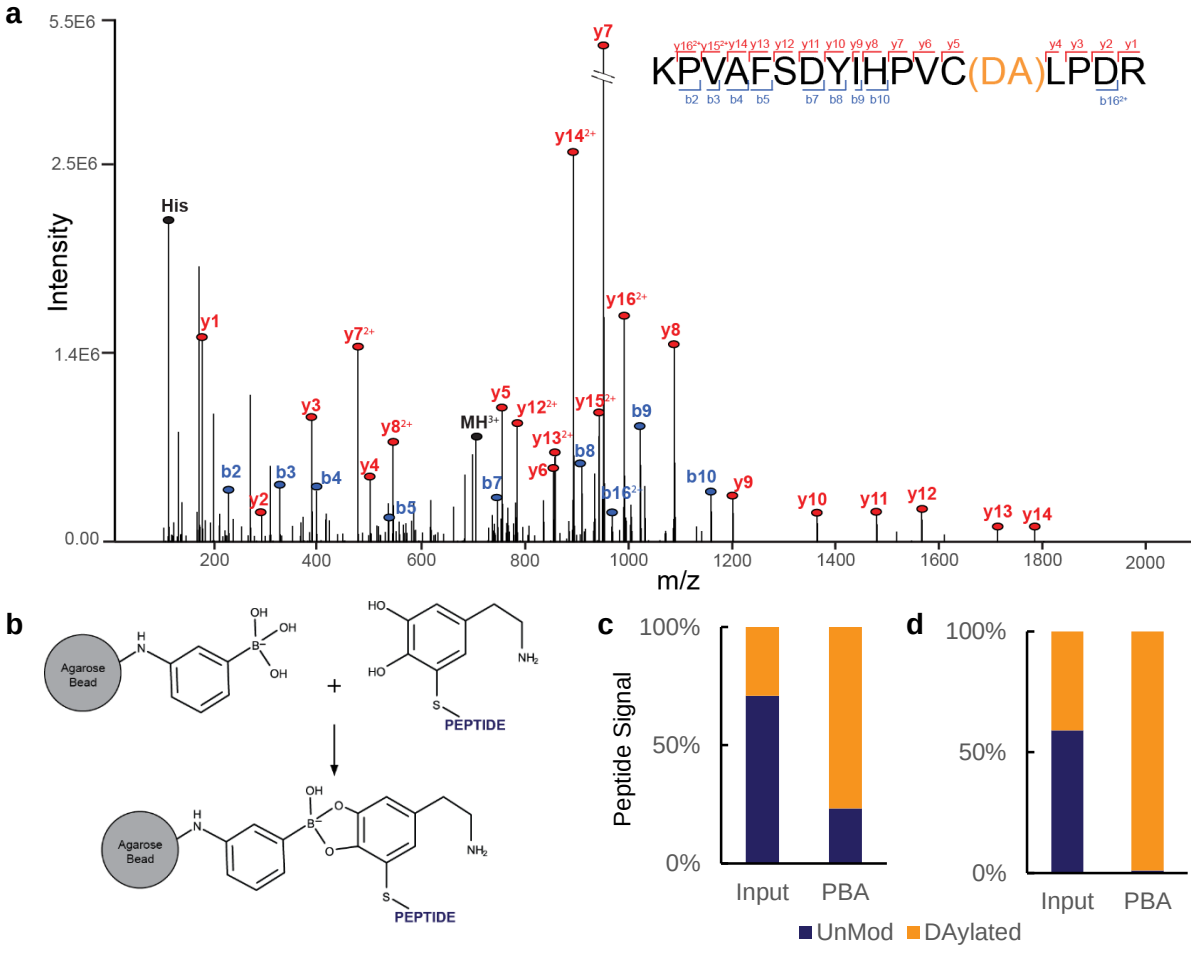

Figure 2.2. Dopaminylated peptide and enrichment a) MS/MS spectra of synthetic peptide treated with 10X molar concentration of DA. Modified cysteine is indicated. **b)** Esterification of boron with the cis-diol moiety with dopaminylated **c)** Percent of contribution to peptide signal from unmodified peptide and DAylated peptide before and after PBA affinity enrichment. **d)** Percent of contribution to peptide signal from unmodified peptide and DAylated peptide before and after optimized PBA affinity enrichment. Optimization lead to nearly 100% of the total peptide signal from DAylated peptides.

2.2.3. Enrichment and identification of *in vivo* dopaminylated peptides

To test our ability to enrich and identify substoichiometric dopaminylated peptides from complex mixtures including cell or tissue lysates, we looked for a cell model that expressed the DA transporters VMAT2 and DAT, were sensitive to DA, and grew quickly. Initially, we used the neuronal cell line SH-SY5Y differentiated with retinoic acid (RA) and 12-*O*-tetradecanoyl-phorbol-13 acetate (TPA) for six days. This differentiation protocol increases expression of dopaminergic markers like tyrosine hydroxylase [85]. However, these cells grow slowly with a doubling time of several days, were difficult to passage, were extremely sensitive to perturbations, and died easily. As an alternative, we utilized a cell model of HEK-293 cells which stably express both DAT and VMAT2, termed HEK-VMAT, from Gary Miller's lab at Columbia University [86]. These cells uptake exogenous DA and have similar doubling times to standard HEK cells, making them a useful cellular model to study protein dopaminylation. Furthermore, these cells can be treated with DA concentrations up to 50 μM without forming melanin pigments or inducing massive cell death.

Our early experiments continued optimizing our DA-modified peptide enrichment method. Optimization was done over 30 biological sample sets, with each set containing dopamine treated and control cells with DA with up to four process replicates. Together, optimization of PBA affinity enrichment from our HEK-VMAT cells model used over 220 LC-MS/MS runs. A summary of these various optimization conditions is included under Methods and an in-depth protocol is included. Briefly, proteins from snap frozen biological samples are extracted in 8 M Urea (100 mM ammonia bicarbonate, 75 mM NaCl, and 5 mM DTT) and sonicated to shear DNA. Proteins were reduced and alkylated, digested, and desalted at 4°C on Waters Oasis Cartridges. Peptides were resuspended in PBA Buffer (30% Acetonitrile (MeCN), 50 mM Phosphate pH 8.5), mixed with PBA beads and incubated for two hours. The bead volume was transferred to StageTip and washed five times with PBA Buffer and eluted with StageTip buffer A (1% MeCN, 0.1% trifluoroacetic acid (TFA)) for 1 hour, followed by an additional wash with 0.1% TFA. We found that performing our washes in a StageTip format increased our reproducibility between process replicates by reducing bead loss compared to batch washes. The eluted fractions were mixed, desalted on StageTips, and analyzed on either a Thermo Orbitrap Elite or Lumos Tribrid mass spectrometer (Figure 2.3A). Raw files were analyzed with variable modifications DA and

Carbamidomethyl (CAM) on cysteine residues. Peptide IDs from the most recent 10 sample sets are summarized in Figure 2.3B, where sets 8, 9, and 10 represent the optimized protocol.

Utilizing our optimized PBA affinity enrichment of dopaminylated peptides, we identified between 800 and 4500 dopaminylated peptides from HEK-VMAT cells treated with 50 μM DA for 24 hours (Figure 2.3B). From each biological sample, we identified between 600-3200 dopaminylated cysteine sites with localization scores greater than 0.75. Our PBA enrichment has low background with over 94% of peptide intensity coming from dopaminylated peptides (Table 2.3). To demonstrate the specificity of our protocol, we also analyzed input whole cell lysates without enrichment. From these unenriched samples, we see fewer than 24 dopaminylated peptides and 15 dopaminylated cysteine sites, which is below our peptide and site ID false discovery rate of 0.01, suggesting that these modified peptides identified from a dataset of 25,450 or 28,222 (unenriched HEK-VMAT 9 or 10, respectively) peptide-spectrum matches (PSM) are likely false-positive PSMs.

Table 2.2: Comparison of enriched and unenriched samples

	Biological Sample	Total # of Peptides	# of DAylated Peptides	# DA Sites	% DAylated Peptides of Peptide Signal
PBA Enriched	HEK-VMAT 8	946	870	658	95.95
	HEK-VMAT 9	1403	1198	901	89.45
	HEK-VMAT 10	4884	4591	3483	98.40
No Enrichment	HEK-VMAT 9	25450	12	15	0.02
	HEK-VMAT 10	28222	24	15	0.06

Next, we questioned if dopaminylation of proteins occurs randomly as this modification is non-enzymatic. A random modification would have equal probability to modify proteins with a solvent exposed cysteine, and would be directly correlated to protein abundance. To interrogate the relationship between abundance and dopaminylation, we overlaid our data from a representative biological replicate (HEK-VMAT 9) onto the proteome of HEK cells. Utilizing the MaxQB database, we extracted the background proteome of HEK cells and ranked proteins by abundance [87]. By overlaying our 481 dopaminylated

proteins detected in this study on the ranked proteins from the MaxQB HEK database, we saw a large portion of our dopaminylated peptides come from highly abundant proteins (Fig 2.3C). However, in the lower two quartiles of proteins ranked by abundance, we identified dopaminylation of 18 proteins. Of these 18, we detected two copper binding amyloid proteins: amyloid precursor protein (APP) and amyloid-like precursor protein 2 (APLP2). APP is processed in the cell to form amyloid-β, the major component of amyloid plaques in Alzheimer's disease. Previous work has shown potential dopaminylation of tyrosine on amyloid-β, but cysteine modification on APP is unknown [88]. Dopaminylation of lower abundance proteins such as these suggests a mechanism that is not restricted to spontaneous DA oxidation resulting in nearby cysteine modification. Unlike other protein modifications like phosphorylation, we were unable to identify a common motif surrounding our dopaminylated cysteine residues (Supplemental Figure 2.1A). It is possible some cysteine residues have microenvironments that make them more likely to be modified, such as proteins which bind redox-active metal ions.

To address the potential of differential susceptibility of cysteine to DA modification, we compared our dopaminylated Cys sites to those identified by LC-MS/MS with two established reactive cysteine probes. These cysteine probes are electrophilic chemical probes used to identify and quantify reactive cysteines; one probe is an iodoacetamide-based chemical probe (IA-alkyne) and applied to cell lysates, while the other is a caged bromomethyl ketone electrophile (caged-BK) which can be used in living cells [89]. We reasoned the caged-BK probe applied to living cells may have a similar cysteine reactivity profile to DA in living cells if dopaminylation is indeed directed by abundance and cysteine availability. We compared our dataset of dopaminylated cysteine sites to reactive cysteines identified using caged-BK probe, and IA-Alkyne (Figure 2.3D). Modified cysteine residues in both DA and caged-BK have only 4.8% overlap; the overlap between DA and IA-Alkyne is 5.9%. These small overlaps suggest dopaminylation may not be a generic modification, but rather some cysteine residues are more prone to specific dopaminylation. The selective dopaminylation of particular cysteines may be important in understanding what role dopaminylation plays under physiological conditions.

Of the 481 dopaminylated proteins we identified in the representative biological replicate (HEK-VMAT 9), 32 are not represented in the MaxQB database for HEK cell line. This may be due to low

expression of these proteins in HEK cells. For example, we identified dopaminylated peptides from our transgenes SLC18A2 (VMAT2) and SLC6A3 (DAT), which normally have low expression in HEK cells [90]. Identification of dopaminylated sites on the DA transporters is especially interesting. In neurons, high expression and activity of VMAT2 has been shown to be neuroprotective against DA oxidation [35]. We found in our HEK-VMAT cells, Cys488 of VMAT2 is dopaminylated (Figure 2.3E). This residue is on the C-terminal tail of VMAT2 and is susceptible to S-glutationylation in the presence of ROS which leads to decreased VMAT activity and impaired DA packaging [91]. Implications of dopaminylation at this site will require further investigation. From the other DA transporter, DAT, we identified two dopaminylations at Cys6 and Cys342 (Supplemental Figure 2.1B,C). Oxidative modifications on Cys342 have been shown to inactivate the transporter and contribute to oxidative stress in DAergic neurons [92]. Cys6 can be S-palmitoylated and is thought to be involved in the function and localization of DAT in neurons [93]. It is possible, given the functional significance of these sites, that dopaminylation of these transporters may alter the homeostasis of DA packaging and increase cytosolic DA, and potentially representing a toxic feed forward mechanism of DA oxidation and oxidative stress.

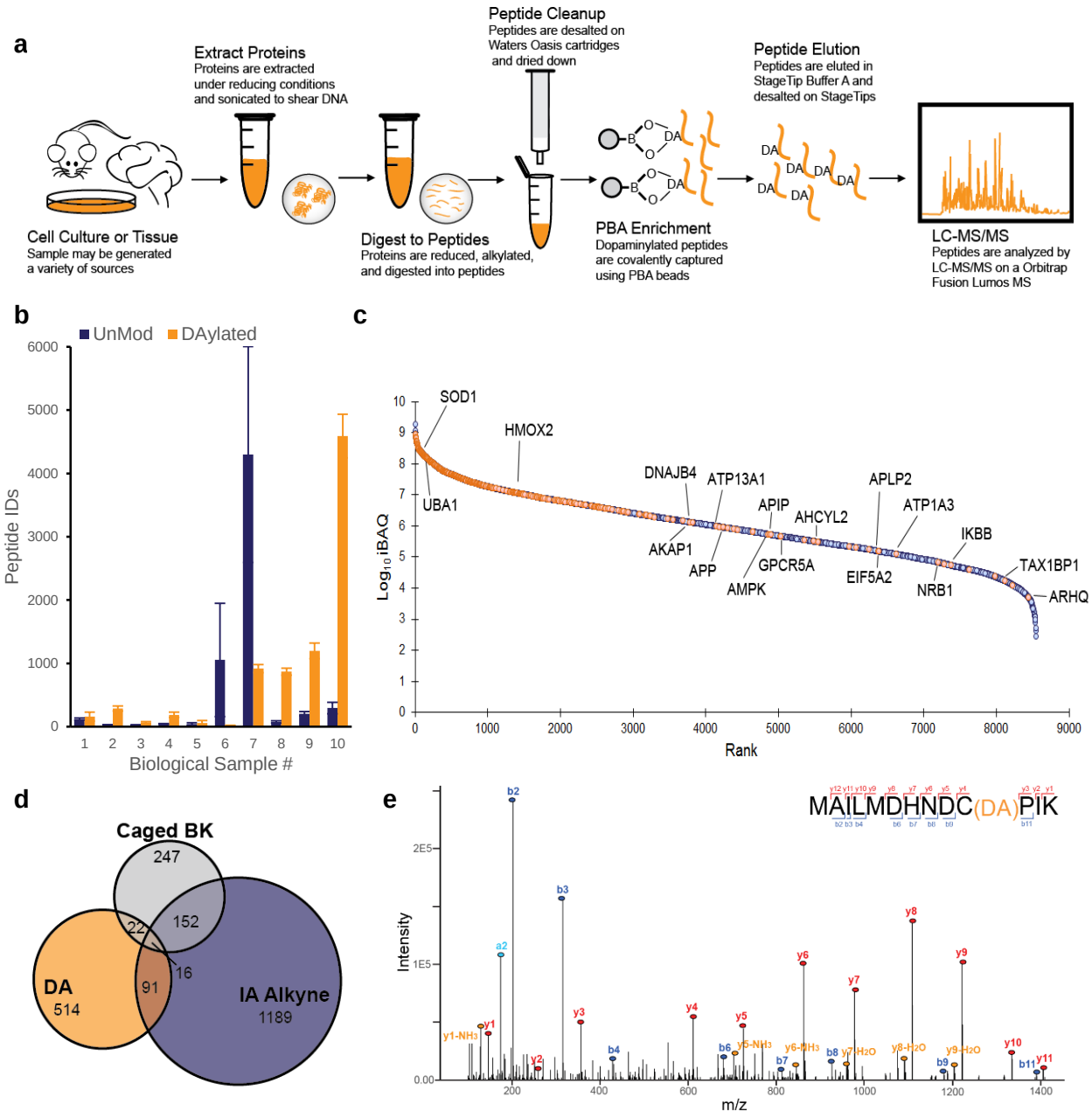

Figure 2.3. Proteins from biological samples are dopaminylated a) Flowchart for the experimental procedure **b)** Peptides identified from 10 biological samples. Samples 8-10 represent the final optimized method with between 800-4500 dopaminylated peptides. **c)** Overlay of identified dopaminylated peptides with MaxQB protein abundance. Orange=DAylated, Blue=Not identified as modified. **d)** Comparison of our dopaminylated cysteines to other electrophilic cysteine probes. **e)** MS/MS of dopaminylated peptide from VMAT2

2.2.4. Enrichment and identification of dopaminylated peptides from human brain

Having established an approach to reliably enrich dopaminylated peptides from a complex cell lysate, we next tested our method with more physiological relevant tissue: human brain. We obtained two control cases and two Lewy body (LB) positive post-mortem, flash-frozen brain tissue samples from the University of Washington Neuropathology Core and subjected them to our boronic acid-based enrichment and LC-MS/MS. We identified over 20 dopaminylated peptides directly from brain (Figure 2.4A). The concentration of cytosolic DA in human neurons is much lower than those used in our HEK-VMAT model system, potentially explaining the reduced number of dopaminylated peptide identifications. Furthermore, our cell line model was optimized to avoid generation of neuromelanin and extensive modifications which are not under our control in human tissue. Further optimization of our protocol may be taken to improve dopaminylated peptide enrichment from complex tissue samples.

Amongst the DA sites identified from human brain tissue, the cysteine residue, Cys147, of superoxide dismutase (SOD1), is consistently found to be dopaminylated in HEK-VMAT cells and in two of four human brain samples, one control and one LB positive (Figure 2.4 B and C, respectively). Interestingly, SOD1 binds both copper and zinc, and copper is linked with DA oxidation and oxidative stress [94]. Furthermore, SOD1 is a key protein involved in detoxification of ROS and oxidative stress and has been studied extensively in neurodegeneration. For example, one previous study demonstrated dopaminylated of SOD1 in differentiated SH-SY5Y cells exposed to DA but was unable to identify the site of dopaminylation [63]. With our method, we identified dopaminylation of Cys147, which forms a critical disulfide bridge at C58-C147. Mutations at Cys147 and subsequent loss of this disulfide bridge promote SOD1 aggregation [94]. Furthermore, SOD1 mutations are key drivers in amyotrophic lateral sclerosis (ALS), a neurodegenerative disorder affecting motor neurons in the brain and lower motor neurons in the brain stem and spinal cord. Whether dopaminylation of SOD1 drives disease or is a consequence of already impaired dopamine homeostasis remains to be determined, but our method will help to elucidate the role of dopaminylation from various biological samples.

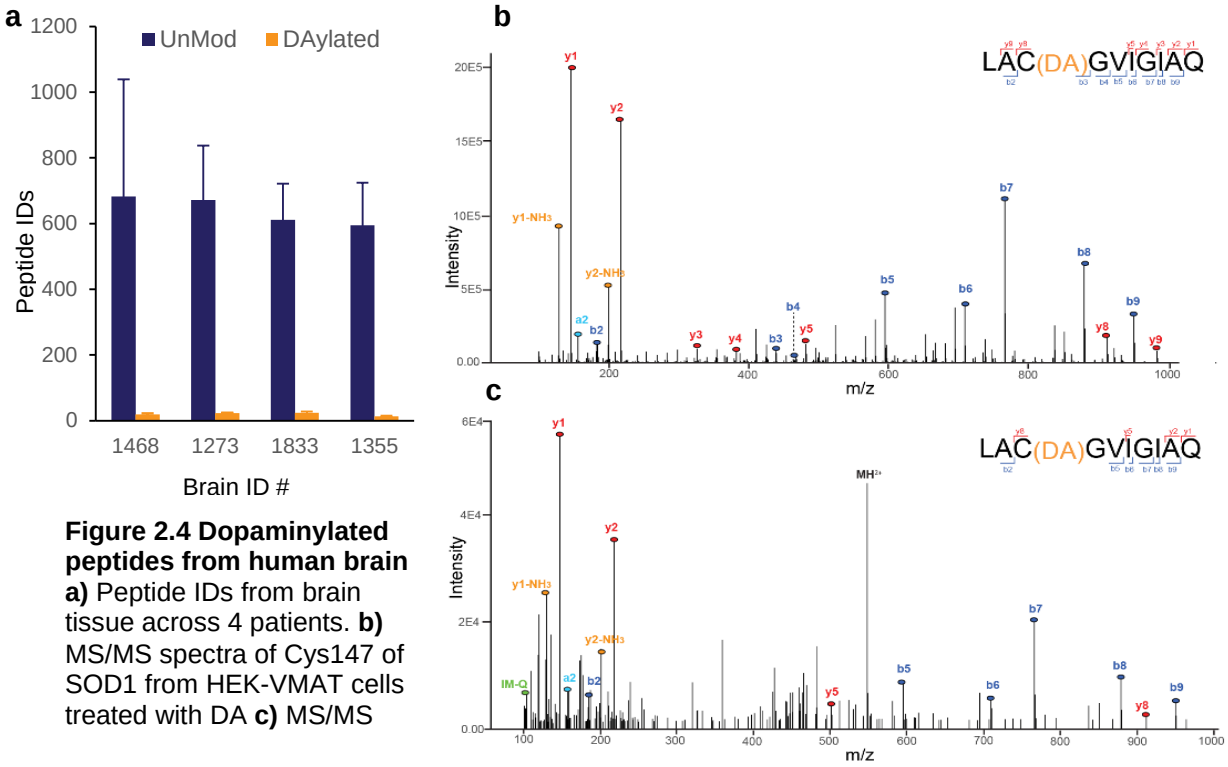

Figure 2.4 Dopaminylated peptides from human brain **a)** Peptide IDs from brain tissue across 4 patients. **b)** MS/MS spectra of Cys147 of SOD1 from HEK-VMAT cells treated with DA **c)** MS/MS

2.3. Materials and Methods

Peptides and Reagents

Peptide standards were purchased from AnaSpec and New England Peptides. Dopamine was purchased from Acros Organics and m-aminophenylboronic acid-agarose was purchased from Sigma.

Protein Labeling and in-Gel Detection

UbE2G1 was gifted by Haibin Mao for early experiments. 5 µg of purified protein was incubated with DA in phosphate buffered saline (PBS) for 96 hours at room temperature. For peroxidase-induced reactions, 5 µg of purified protein was incubated with DA, IgG-HRP (Sigma), and 2 mM H_2O_2 for 25 minutes. Experiments were also carried out in 50mM Tris buffer, pH 7.4, which may increase DA oxidation. Reactions were quenched by adding 4X Bolt LDS Sample Buffer (Thermo) supplemented with 5 mM DTT. Proteins were analyzed by sodium dodecyl sulfate-polyacrylamide gel electrophoresis (SDS-PAGE). Gels were scanned on an Odyssey infrared imager (Li-Cor Biosciences, ex = 685 nm) and quantified in Adobe Photoshop. Total protein was visualized by staining with colloidal blue coommassie and imaged on a FluorChem E imager.

Peptide Labeling and Enrichment

Peptides were dissolved to 100-500 µM in PBS and incubated with equimolar fresh DA for 96 hours at room temperature. The reaction was stopped by addition of 10% TFA to acidify peptide mixtures, and desalted using StageTips [95] and analyzed by LC-MS/MS. The stoichiometry of peptide dopaminylation was calculated by integrating the area under the curve for the monoisotopic mass of the modified peptide rationed to the unmodified peptide. A mass window of +/-0.3 amu was allowed, and the ICIS peak detection algorithm feature of Xcalibur was used for automated detection of peaks.

Identification of Dopaminylated Peptides from cell culture

HEK293 cells stably expressing VMAT2 and DAT were gifted by Dr. Gary Miller (Columbia University). Cells were grown in DMEM media supplemented with 10% FBS (Hyclone, GE) and Penicillin-Streptomycin-Glutamine (100X, Thermo Scientific), 100 µg/ml Zeocin (Invitrogen) and 250 µg/ml G-418 (GoldBio) in an incubator at 37°C and 5% CO_2.

Cells were plated in six 15 cm dishes and grown to 60% confluence. Fresh media (20 mLs) was added 16-18 hours prior to DA treatment (the day before). Three of six plates were treated with either 10 or 50 µM DA for 24 hours. DA was made at 1000x stock in PBS and aliquots were stored at -80°C. It is important to avoid freeze/thaw cycles as DA will oxidize quickly. After treatment, cells were washed 3X with 20 mls of ice-cold PBS. An additional 1 mL of cold PBS was added to dishes and cells are scraped with a rubber spatula and collected in a 15 mL conical vial. Cells were kept on ice while untreated dishes were collected. Cells were pelleted via centrifugation for 2 min at 2,325 x g. The supernatant was aspirated and cell pellets snap frozen in liquid nitrogen. Cell pellets were stored at -80°C until ready to process.

Frozen cell pellets were lysed in 1.5 mL of 8 M Urea (100 mM ammonia bicarbonate, 75 mM NaCl, 5 mM DTT). Pellets were broken up by pipetting up and down with P-1000 until clumps dissolved. The lysate was transferred to a low-retention 2 mL microcentrifuge tube and sonicated in a Cup Horn sonicator (QSonica) for 20 minutes (30s on/off). The sonication cup must be filled with ice and replenished after 10 minutes to keep samples cold. Lysates are clarified by centrifugation at 21,000 x g and 4°C for 10 minutes. Soluble protein fractions were transferred to a fresh microcentrifuge tube.

The protein content was measured using Pierce 660 nm Assay Reagent (Thermo Scientific) using a BSA standard curve. 8 mg (4 process replicates of 2 mg each) of protein was transferred into a 15 mL conical vial. Proteins were reduced with 1 mM TCEP for 10 minutes at room temperature and alkylated with 10 mM chloroacetamide for 45 minutes at room temperature in the dark. Proteins were diluted 2-fold with 50 mM Tris pH 8 and digested with LysC (Wako Chemicals) at 1:100 for 2 hours at room temperature. Proteins are diluted further until Urea < 1.5 M, and digested with Trypsin (Thermo Scientific) at 1:100 at room temperature while shaking overnight. In morning, another 5 µg trypsin was added and incubated for 1 hour. Samples were acidified to pH 2 with 10% TFA. Any insoluble proteins were pelleted by centrifuging samples at 5000 x g for 5 minutes and then placed on ice. Peptides were then extracted with Oasis HLB 3cc 60mg cartridges at 4°C in a cold room. Cartridges were conditioned with 3 mL of 100% MeCN, followed by 3 mL StageTip Buffer B (50% MeCN, 0.1% TFA), and washed two times with 3 mL StageTip Buffer A (1% MeCN, 0.1% TFA). Peptides are loaded on the cartridges and washed two times with cold StageTip Buffer A. Cartridges were moved back to room temperature, and peptides are

eluted two times with StageTip Buffer B into two 2 mL microcentrifuge tubes. Peptides were dried to completion using a Thermo Scientific Speedvac (about 4 hours). Dried peptides were stored at -80°C.

Peptides were resuspended in 800 µL PBA Buffer (30% MeCN, 50 mM Phosphate pH 8.5) and bath sonicated for 5 minutes to help dissolve peptides. Peptides were clarified via centrifugation at 14,000 x g for 5 minutes and transferred to a new tube. While peptides were cleared by centrifugation, 2x 40 µL of m-aminophenlyboronic acid-agarose (PBA) (10 µL for each 2mgs of peptide) were aliquoted into low retention 1.5 mL microcentrifuge tubes. Beads were mixed prior to pipetting. PBA beads were washed with 1 mL 30% MeCN, 0.1% TFA for 5 minutes, centrifuged for 30s on a tabletop centrifuge, and allowed beads to settle for 5 minutes. The supernatant was removed and beads were primed with 1 mL 100mM Phosphate Buffer pH 10 for 5 minutes, centrifuged for 30s on a tabletop centrifuge, and beads allowed to settle for 5 minutes. The supernatant was discarded. 400 µL PBA buffer was mixed with beads and aliquoted into four 1.5 mL microcentrifuge tube using a cut, widebore P-200 pipette tip. 200 µL of peptides was added to beads and incubated for 2 hours with end-over-end rotation.

While peptides and PBA beads incubated, StageTip were made by adding two plugs of C18 to P-200 pipette tips. These were used as fritted columns to wash beads.

Peptide/PBA bead mixtures were collected via tabletop centrifuge and ~80% of the supernatant was removed. The remaining mixture was transferred StageTips and centrifuged using StageTip adaptors to remove remaining liquid. Caution must be used to avoid the beads drying. PBA beads were washed with 400 µL PBA buffer five times and centrifuged to remove supernatant. Extended pipette tips were used when adding washes to mix beads and PBA Buffer each time to ensure adequate washing. Peptides were released from PBA beads by adding 300 µL StageTip Buffer A and incubating for one hour. The elution was collected by centrifugation into a fresh microcentrifuge tube. An additional 300 µL of 0.1% TFA was added to PBA beads and incubated for 20 minutes and centrifuged to collect elution. Finally, 30 µL of 35% MeCN 0.1% TFA was added (to elute peptides bound to C18 plug). These three elutions were combined and desalted on StageTips at 4°C. Briefly, each StageTip contains two plugs of Empore SDB-XC. StageTips were conditioned with 50 µL MeOH, 50 µL StageTip Buffer B (50% MeCN, 0.1% TFA), and two 50 µL washes of StageTip Buffer A (1% MeCN, 0.1% TFA). Peptides were added

and bound. StageTips were washed with 100 µL of cold StageTip Buffer A followed by elution by 50 µL 35% MeCN 0.1% TFA. Peptides were then dried via speedvac and resuspended in StageTip Buffer A.

LC-MS/MS

Peptides were separated on a Thermo EASY-nLC 1200 UHPLC instrument (Sunnyvale, CA) with 10 cm long fused silica capillary columns made in-house with a laser puller (Sutter, Novato, CA) and packed with 3 µm 120 Å reversed phase C18 beads (Dr. Maisch, Ammerbuch, DE). The LC gradient was 133 min long with 4–38% B at 200 nL/min. LC solvent A was 0.1% acetic acid and LC solvent B was 0.1% acetic acid, 80% acetonitrile. MS data was collected with a Thermo Orbitrap Fusion Lumos Tribrid mass spectrometer. Data-dependent analysis was applied using Top15 selection with HCD fragmentation with 31% HCD collision energy. Raw files were analyzed by MaxQuant/Andromeda [72] version 1.5.2.8 using protein, peptide and site FDRs of 0.01 and a minimum score of 40 for modified peptides, 0 for unmodified peptides; minimum delta score of 17 for modified peptides, 0 for unmodified peptides. MS/MS spectra were searched against the UniProt human database (updated July 22nd, 2016). MaxQuant search parameters: Variable modifications included Oxidation (M), Carbamidomethyl (C), and Dopaminylation (C). For dopaminylation, the chemical formula was C(8) O(2) N H(9) and a mass of 151.0633 g/mol. Max. labeled amino acids was 3, max. missed cleavages was 2, enzyme was Trypsin/P, max. charge was 7. The initial search tolerance for FTMS scans was 20 ppm and 0.5 Da for ITMS MS/MS scans. Data and raw spectra were analyzed in Excel, R, and Perseus. Modified peptides were only considered identified if MaxQuant is able to compute a peptide intensity in three process replicates (of four).

2.4. Discussion

Protein and peptide dopaminylation is an important but understudied PTM. Currently, the functional significance of increased cytosolic DA is unknown although studies suggest cytosolic DA is important for neurodegenerative disease. The role that DA plays in neurodegeneration is linked to oxidative stress as unregulated DA quickly forms reactive oxidation products like DAQ, which may modify proteins. Modification of proteins occurs at physiological pH; therefore it is possible to dopaminylate proteins both in the cytosol and extracellular matrix when DA is released into the synapse. While in most cases cytosolic DA concentrations remain low, the presence of NM suggests there is adequate cytosolic DA that eludes standard antioxidants like glutathione to allow the formation of complex, DA-protein aggregates. Unbiased tools to characterize dopaminylation are critical to advance this field and elucidate the functional significance of this PTM.

We describe a new method for direct detection of protein dopaminylation utilizing boronic-acid based enrichment and LC-MS/MS. Our data indicates that our enrichment protocol yields 450-fold increase of peptide signal from dopaminylated peptides which are undetectable without enrichment. For dopaminylated peptides which are detected pre and post-enrichment, we see a 208-fold increase in peptide signal after PBA enrichment. We employed our protocol to identify 1860 dopaminylated proteins with roughly 3400 unique dopaminylated cysteine residues in HEK-VMAT cells treated with DA. Several of these proteins have been previously described as DA-modified, though our method now provides specific site identification of DA modifications. Identification of sites is critical to elucidate the functional consequence of DA modifications. For example, we identify Cys 488 of VMAT2 as dopaminylated. Previous work has shown that under oxidative stress, this site can be modified by glutathione and slows VMAT2 activity [91]. To our knowledge, this is the first report to find DA modification of VMAT2.

Unlike other methods which employ radioactive DA or purified proteins, the method described in this study translated to study human tissue or fluids. Here, we show that from four clinical patient samples, we can identify 20 dopaminylated sites, including Cys146 of SOD1. Cys146 of SOD1 forms a critical disulfide bridge and loss of this bridge promotes protein aggregation [94]. Currently, the role of

dopaminylation in SOD1 aggregation is unknown, but our findings suggest a potential mechanism and further study is needed.

The method described here should also facilitate the study the effect of dopaminylation and the consequences in DA neurons. We believe our method can be used to study range of neurotoxic effects due to DA, from neurodegeneration to pesticide-induced toxicity.

2.5. Supplemental Figures

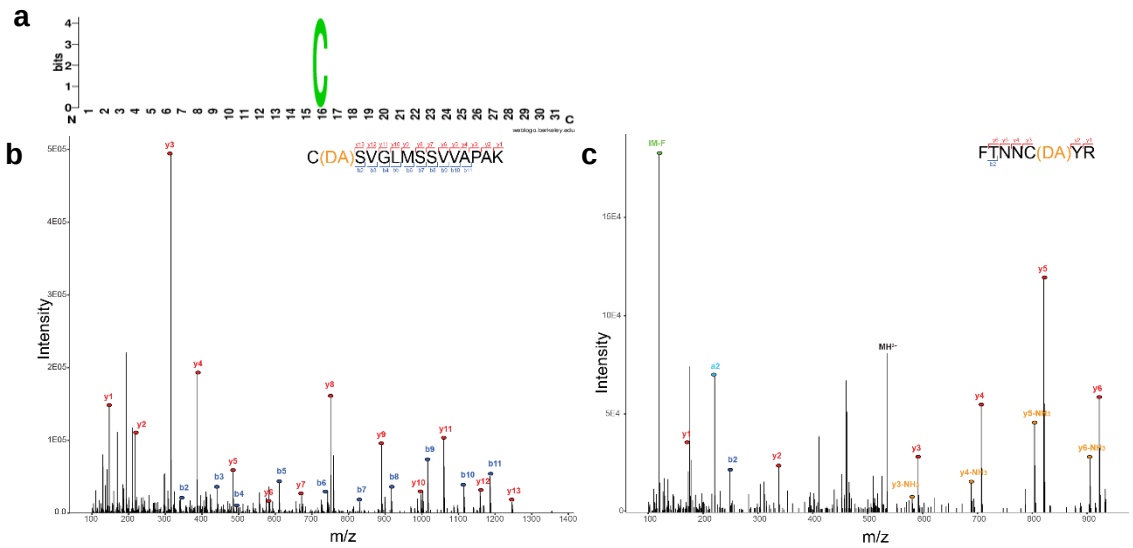

Supplemental Figure 2.1 Additional dopaminylated peptides a) Sequence Logo **b)** Dopaminylated Cys 6 of DAT **c)** Dopaminylated Cys 342 of DAT

2.6. Acknowledgements

We are grateful to Haibin Mao for his generous gift of UbE2G1 and CDC34 purified proteins, Gary Miller for generously supplying the HEK-VMAT cell lines, and Dr. Dirk Keene for human brain tissue and discussion. This work was supported by Molecular Pharmacology Training Grant.

3.1. Introduction

The repertoire of tools is limited to study the dopaminylation of proteins and peptides as a post-translational modification (PTM). Other PTMs like phosphorylation or ubiquitylation can be studied using antibodies which have been developed against the PTM itself. For example, antibodies for phospho-tyrosine detect global phosphorylation of tyrosine independent of protein sequence and may be used for unbiased study of tyrosine phosphorylation [96]. However, reliable antibodies have not been developed for dopaminylation and, therefore, even common antibody-based techniques like Western blotting and immunofluorescence (IF) are unavailable. To address this, we proposed an alternative strategy to investigate dopaminylation: a modified dopamine containing a biotin group. If biotinylated dopamine (BD) underwent oxidation and modified proteins as DA does, the suite of avidin-based enrichment tools would be available to study dopaminylation. The interaction between biotin and avidin is strong and can be utilized to enrich biotinylated proteins for MS analysis, and used for Western blots or IF. Other groups have taken advantage of a similar mechanism using a genetically modified peroxidase (APEX) to catalyze the covalent addition of proteins with biotin-tyramide [97]. Biotin-tyramide is similar in structure to BD except for the additional hydroxyl group on BD, however biotin-tyramide requires a peroxidase to biotinylate proteins. The APEX strategy has been used to identify the mitochondrial proteome, the cilia proteome, and proteins at a specific genomic loci using various avidin-based tools [97-99]. Therefore, we believe avidin-based tools can be adopted for use with BD to study dopaminylation in cell models.

Another alternative method we explored was the use of near-infrared (nIRF) imaging of dopamine-protein modifications. Dopaminylated proteins exposed to oxidative conditions can undergo further oxidation from to form protein-dopamine *o*-quinone (DAQ-protein). These o-quinones have specific excitation-emission properties in the nIRF range and can be detected using a Li-Cor Odyssey infrared imager [82]. We hypothesized that this approach can be adapted using a confocal microscope with nIRF capabilities and will discuss our findings in this chapter.

3.2. Results

3.2.1. Biotin-dopamine

To determine if a biotinylated dopamine strategy was feasible, we used biotin-dopamine (BD) to compare to with our work on dopaminylation. The structure of BD maintains the reactive catechol group but substitutes a biotin group on the primary amine (Figure 3.1A). The addition of a biotin group to dopaminylation was attractive because it allows us to utilize the suite of avidin-based technology to study dopaminylation.

To determine BD reactivity, we tested three concentrations of BD on our test protein, UbE2G1, for 96 hours. After Ponceau staining to visualize total protein, a faint band at 40 kDa after incubation with 125 μM BD was visible, but this effect was lost with decreasing concentration of BD (Figure 3.1B left). This suggests that at higher concentrations, BD is able to crosslink UbE2G1 to form dimers in a concentration dependent manner similar to DA but less efficiently (in comparison with Figure 2.1B). Next, we probed our membrane with avidin-HRP to detect BD modifications of UbE2G1 (Figure 3.1B right). We saw strong evidence of BD modification of UbE2G1 in both 125 and 12.5 μM BD. Additionally, we detected BD signal at 40 kDa and 60 kDa, suggesting multimerization of UbE2G1 in the presence of BD. Next, we treated our standard peptides (Table 2.1) with BD and detected modification on Cys residues (Figure 3.1C). From these results we reasoned that BD may have slower rates of polymerization needed for crosslinking, however BD has similar reactivity to DA to modify cysteine residues of proteins and peptides.

Next, we reasoned that BD may cross cell membranes because BD is not charged, unlike DA which carries a plus charge on the primary amine at physiological pH and requires specialized transporters. We treated a mouse neuroblastoma (N2A) cell line with five concentrations of BD for 96 hours and saw increasing biotin-dopaminylation of proteins with increasing BD concentrations (Fig 3.1D). We also saw a similar, concentration dependent increase in biotin-dopaminylation in human neuroblastoma cells (SH-SY5Y) (Supplemental Figure S3.1A). This suggests BD is oxidized in cells and modifies proteins. Interestingly, we found that biotin-tyramide, which lacks a second hydroxyl group, does not spontaneously modify proteins at the same concentrations (Supplemental Figure S3.1B). Finally, to optimize conditions, we treated N2A cells with 50 μM BD and detected biotin-dopaminylated proteins after

30 minutes (Supplemental Figure S3.1C). We see that the banding pattern between six and 24 hours is similar, with signal loss at 48 hours. Therefore, we chose 24 hours for BD treatment in further experiments.

To determine if biotin-dopaminylation was localized in the cell, we carried out immunofluorescence on N2A cells treated with BD for 24 hours. Biotin-dopaminylation appears to be absent in the nuclei and localized throughout the cells. We note that BD localizes near but is not completely constrained to the mitochondria (Fig 3.1E).

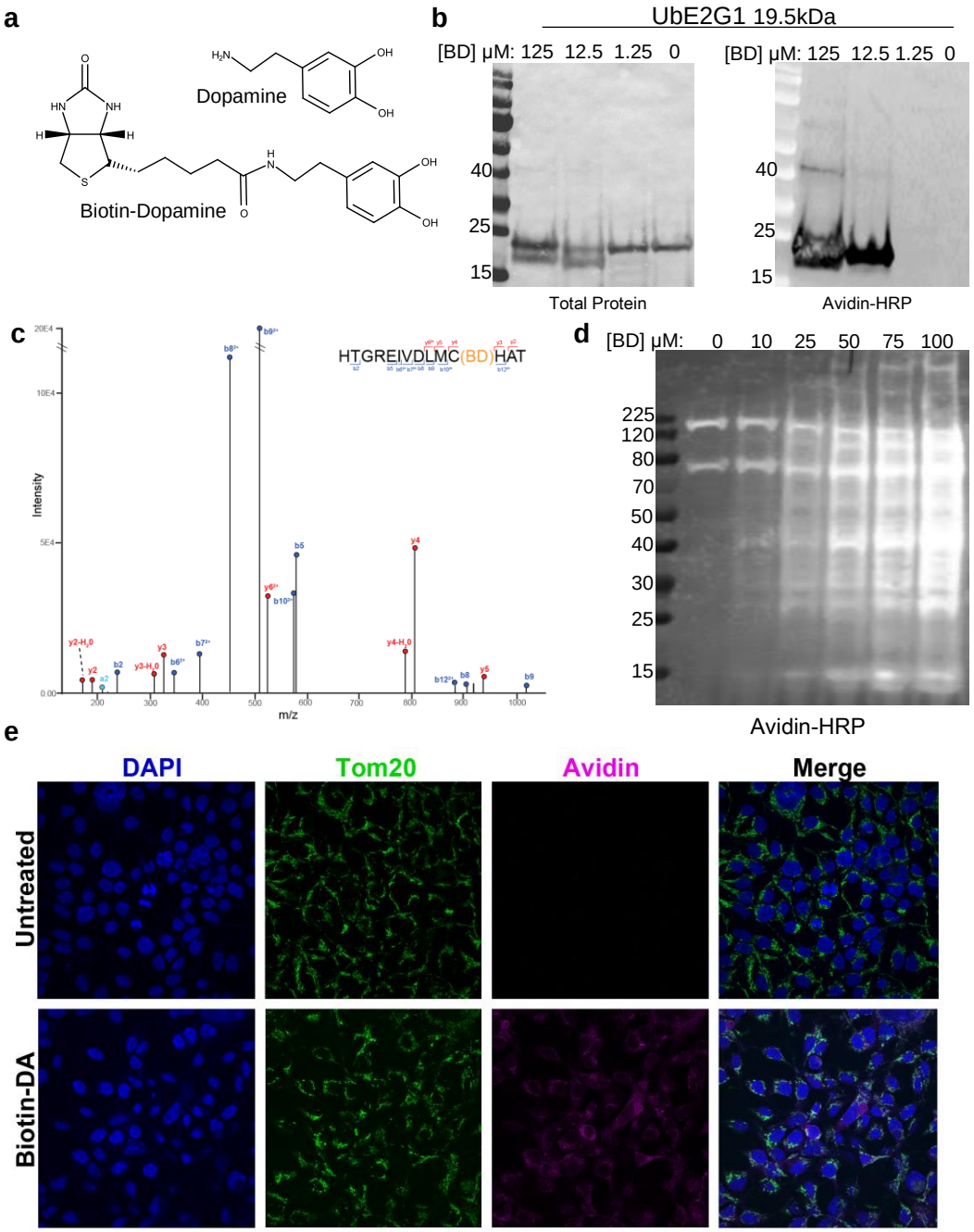

Figure 3.1. Biotin-dopamine modifies peptides and proteins a) Chemical structure of dopamine and biotin-dopamine **b)** UbE2G1 treated with biotin-dopamine for 96 hours at room temperature. Left: Ponceau Stain, Right: Avidin-HRP **c)** MS/MS spectra of biotin-dopamine modified peptide **d)** Western blot of N2A cells treated with increasing concentrations of BD for 96 hours **e)** Immunostaining of control and BD-treated N2A cells with actin (green) and avidin (magenta). Nuclei are shown in blue.

Finally, to identify biotin-dopaminylated proteins, we utilized streptavidin-based enrichment coupled with label-free quantitative proteomics. We identified 105 unique proteins by MS, 97 of these are significantly enriched across two biological replicates of N2A cells treated with 50 μM compared to untreated controls (Figure 3.2A). We find several proteins previously implicated in neurodegenerative disease enriched in BD treatment such as proteins found in amyloid plaques or Lewy Bodies including MAPT, GPHN, and RTN3, as well as other proteins associated with neurodegeneration including: CAMK2G, CISD2, PPP5C, and HMOX2 [100-106]. Proteins involved in protein homeostasis were also found to be significantly enriched with biotin-dopamine treatment. For example, BAG3 functions as a co-chaperone with HSP70 and HSPB8 under acute stress and in cellular aging to degrade proteins via macroautophagy [107]. Furthermore, BAG3-mediated protein degradation is critical for aggregation-prone proteins implicated in various neurodegenerative disorders.

Curiously, we identified several proteins that were not significantly enriched after BD treatment despite their known sensitivity to oxidative modifications. For example, the peroxiredoxins (PRDX) family of proteins are not significantly enriched in BD (shown in purple). Peroxiredoxins are abundant enzymes in mammalian cells that use their redox-active cysteine to neutralize oxidative species and modulate oxidative stress [108, 109]. Another protein family we identified but was not enriched was the heat-shock (HSPs) chaperone family (shown in green). These molecular chaperones protect against oxidative stress, regulate redox homeostasis, and have been shown to be oxidative modified in neurodegeneration [110, 111]. As both PRDXs and HSPs are abundant, sensitive to changes in oxidation, and are known to undergo oxidative modifications, it is curious that these enzymes are not susceptible to biotin-dopaminylation.

To determine if biotin-dopaminylation is related to abundance, we compared our biotin-dopaminylated proteins with the proteome of N2A cells. We ranked the proteome using the extracted iBAQ values from MaxQB and plotted the rank and iBAQ values (shown in blue). We then colored our identified biotin-dopaminylated proteins in orange (Fig 2.2B). Of the 97 proteins identified to be biotinylated by BD, eight are in the lower half of the abundance rank.

Last, we compared our biotin-dopaminylated proteins to our dopaminylated proteins from our PBA enrichment experiments. We see that very few proteins appear in both conditions (Fig 3.2C). Of the 18 which appear in both conditions, HMOX2, ATP13A1, and BAG3 are associated with neurodegeneration.

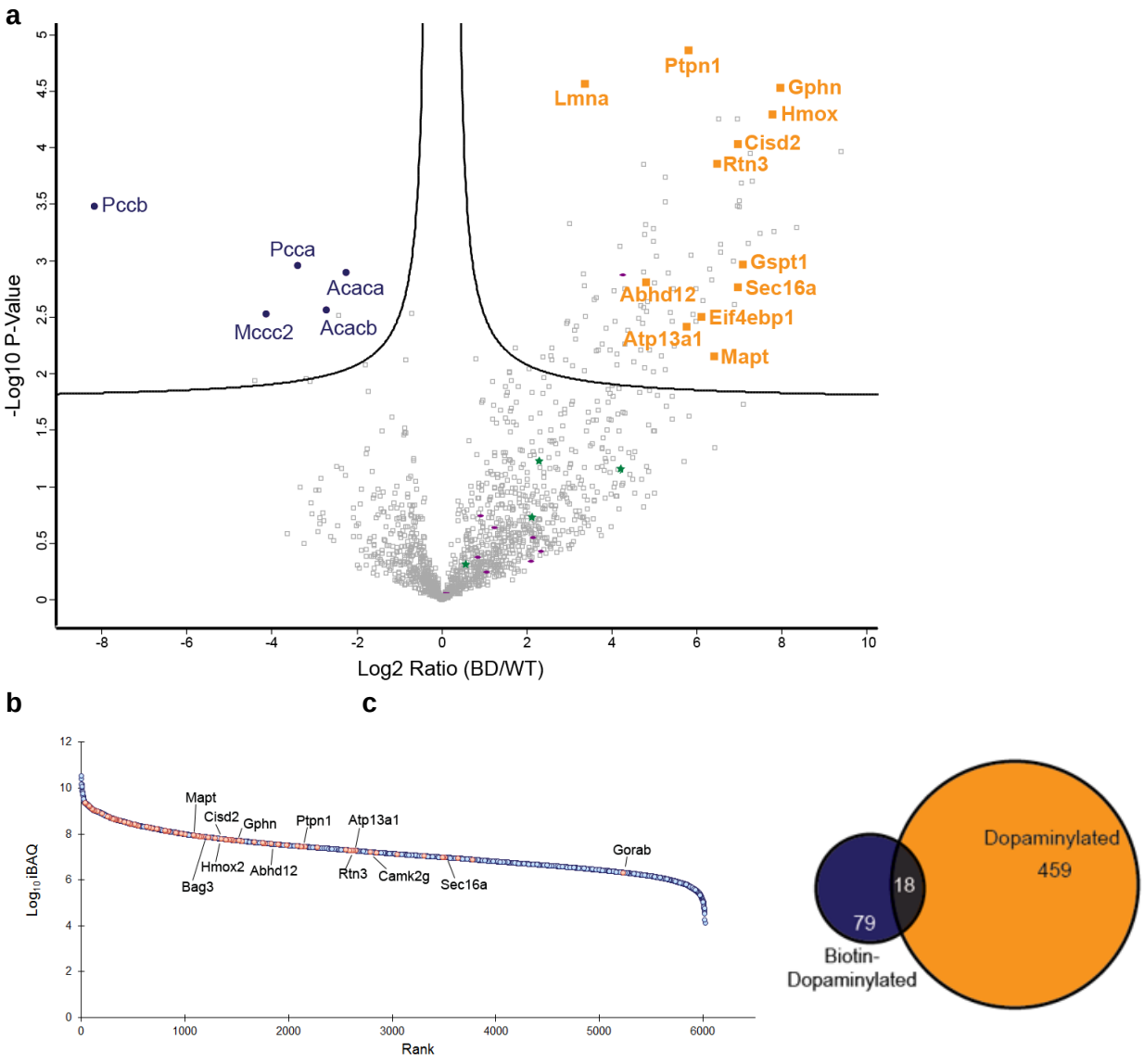

Figure 3.2. Biotin-dopamine differentially modified proteins in N2A cells. a) Distribution of biotinylated proteins from no treatment (WT) and 50 μM BD treatment (BD). Volcano plot shows proteins significantly enriched via streptavidin pull-down. T-test performed in Perseus. Proteins are distributed along x-axis by Log2 Ratio of BD/WT and along the y-axis by p-value. Orange: Proteins implicated in neurodegeneration. Blue: endogenously biotinylated proteins. **b)** Overlay of Biotin-dopamine modified proteins with protein abundance from N2A cells. Orange= Biotin-dopaminylated, Blue=Not identified as modified. **c)** Venn diagram of protein names identified as biotin-dopaminylated in N2A or dopaminylated in HEK-VMAT (Chapter 2, Replicate 9)

We also tested our BD approach in differentiated SH-SY5Y cells. SH-SY5Y cells treated with retinoic acid and 12-O-tetradecanoyl-phorbol-13 acetate for three days each show increased cell projections and are reported to be more “dopaminergic-like” [18]. After differentiation, cells we incubated with 50 μM of BD for 24 hours, lysed, and biotinylated proteins were enriched via streptavidin beads. Proteins were digested off beads and peptides were analyzed by LC-MS/MS. We detected 830 proteins significantly enriched with BD treatment (Figure 3.3A). Proteins found in amyloid plaques or Lewy Bodies (mentioned above) were also found enriched after BD treatment. Next, we compared proteins found to be biotin-dopaminylated to our dopaminylation data sets and found 12% of proteins we identified are modified by both BD and DA (Figure 2.3B). This low overlap may be due to differences in protein expression and solvent exposed Cys across cell types and/or differential electrophilic characteristics between DA and BD.

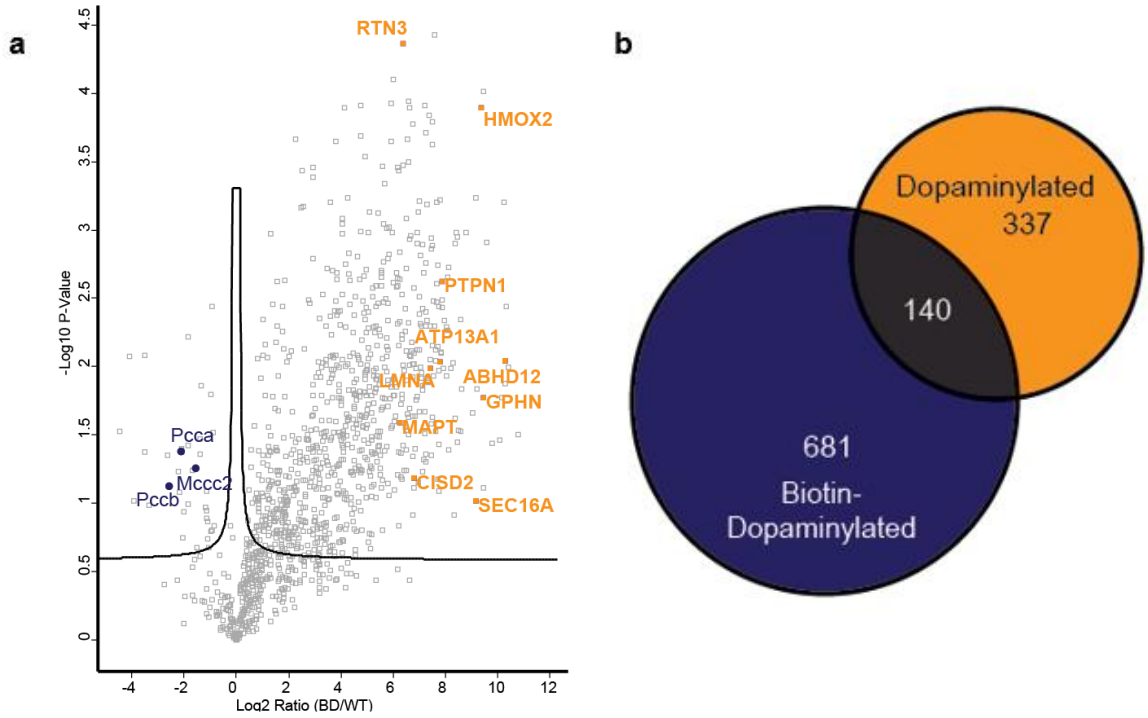

Figure 2.3. Biotin-dopamine differentially modified proteins in differentiated SH-SY5Y cells
a) Distribution of biotinylated proteins from no treatment (WT) and 50 uM BD treatment (BD) in differentiated SH-SY5Y cells. Volcano plot shows proteins significantly enriched via streptavidin pull-down. T-test performed in Perseus. Proteins are distributed along x-axis by Log2 Ratio of BD/WT and along the y-axis by p-value. Orange: Proteins implicated in neurodegeneration. Blue: endogenously biotinylated proteins. **b)** Venn diagram of protein names identified as biotin-dopaminylated in SH-SY5Y cells or dopaminylated in HEK-VMAT cells (Chapter 2, Replicate 9)

3.2.2. nIRF confocal imaging

After verifying our ability to detect the quinone group of dopaminylated proteins (Figure 2.1E), we next tested whether this same technology can be applied using a confocal microscope with fixed tissue. To ensure high levels of dopaminylation, we first treated fixed and permeabilized HEK-VMAT cells with DA under ambient oxygen or with equimolar H_2O_2 for 2 hours. Previous experiments suggested that polydopamine and neuromelanin are not detected using nIRF (not shown), therefore we used the same concentrations of DA as our live-cell DA treatments to avoid creating visible discoloration. Post DA incubation, cells were stained with DAPI and Actin-Green and imaged on a Leica SP8X Confocal Microscope (Figure 3.4A). In slides treated with DA, we are able to detect signal in the nIRF channel, which appears to be punctate-like (indicated with arrows). Next, we used cells treated with DA in culture before fixing and staining. Here, HEK-VMAT cells were treated with 50 μM DA for 24 hours before fixing and staining with DAPI and an anti-DAT antibody (Figure 3.4B). Here, there is increased fluorescence intensity from dopaminylation in cells treated with DA, suggesting confocal imaging utilizing nIRF can be used to visualize dopaminylation in fixed samples.

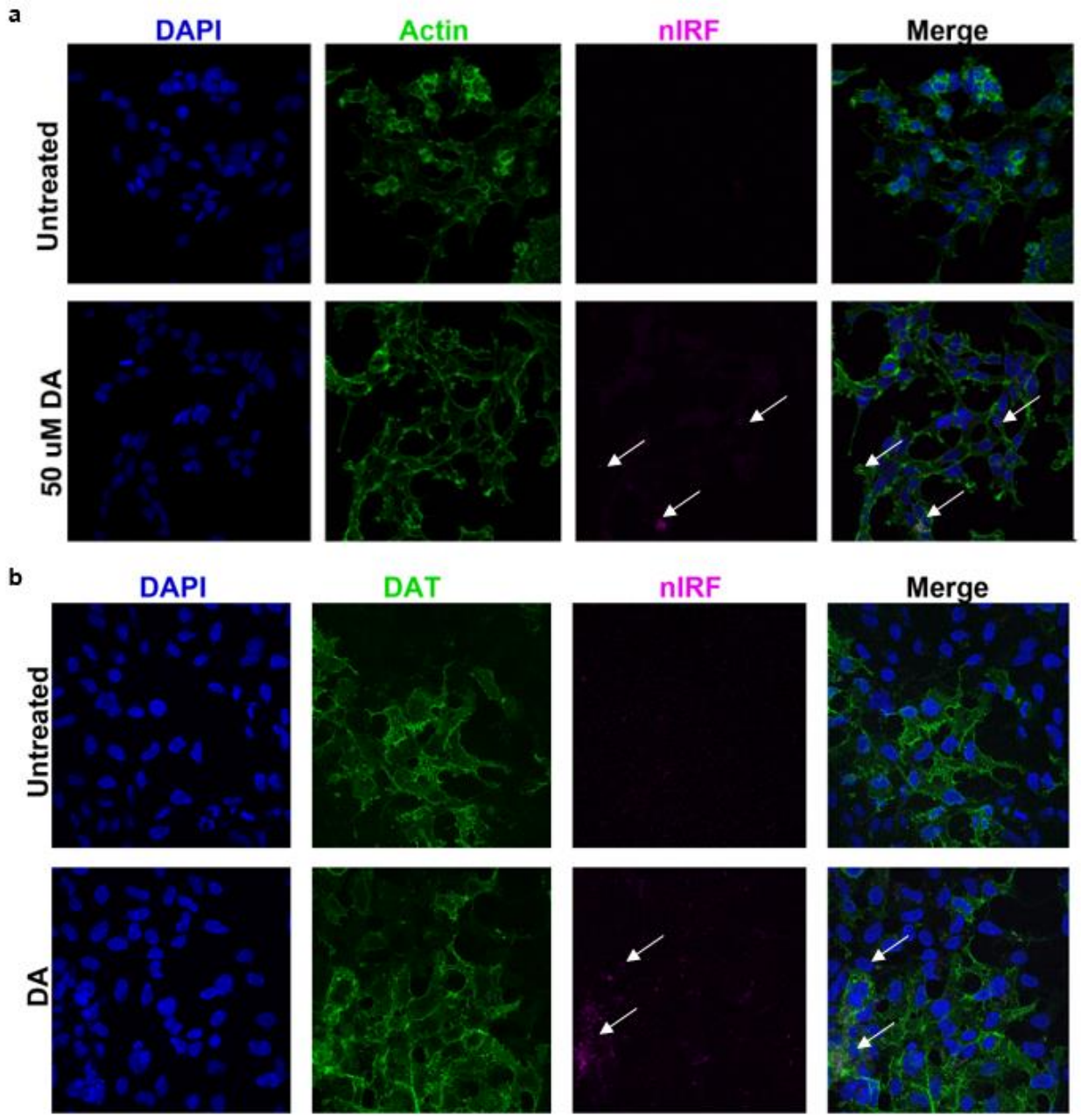

Figure 3.4. nIRF detection of dopamine quinones in HEK-VMAT cells a) Immunostaining of HEK-VMAT cells fixed, permeabilized and treated with DA before staining. Green is actin, magenta is nIRF signal from o-quinones. Nuclei are shown in blue. Arrows show areas of increased nIRF signal **b)** Immunostaining of HEK-VMAT cells treated with DA before cells were fixed, permeabilized and stained. Green is DAT, magenta is nIRF signal from o-quinones. Nuclei are shown in blue. Arrows show areas of increased nIRF signal

3.3. Materials and Methods

Peptides and Reagents

Peptide standards were purchased from AnaSpec and New England Peptides. Dopamine was purchased from Acros Organics and biotin-dopamine was purchased from SynInnova. For protein visualization, antibodies were purchased from Santa Cruz Biotechnologies: Tom20 (sc-17764), Sigma: DAT (MAB369), Avidin-FITC (A2050), and Avidin-HRP (A7149), Invitrogen: ActinGreen 488 (R37110), NucBlue (R37606), and Goat Anti-Rabbit Alexa 555 (A27039). NanoLink Streptavidin Magnetic beads were purchased from Solulink.

Protein Labeling and in-Gel Detection

UbE2G1 was gifted by Haibin Mao for early experiments. 5 µg of purified protein was incubated with BD in PBS for 96 hours at room temperature. Reactions were quenched by adding 4X Bolt LDS Sample Buffer (Thermo) supplemented with 5 mM DTT. Biotin-Dopaminylation was detected by Western Blot with avidin-HRP (1:5000, Sigma A7149). Proteins were visualized by staining with ponceau stain and imaged on a FluorChem E imager.

Peptide Labeling with BD

Peptides were dissolved to 100-500 µM in PBS and incubated with BD for 96 hours at room temperature. The reaction was stopped by addition of 10% TFA to acidify peptide mixtures, and desalted using StageTips. Analysis was performed by LC-MS/MS. The abundance of modified peptides was calculated by integrating the area under the curve for the monoisotopic mass of the modified and unmodified peptide. A mass window of +/-0.3 amu was allowed, and the ICIS peak detection algorithm feature of Xcalibur was used for automated detection of peaks.

Enrichment and Identification of Biotin-Dopaminylated proteins

N2A cells were grown in DMEM media supplemented with 10% FBS (Hyclone, GE) and Penicillin-Streptomycin-Glutamine (100X, Thermo Scientific) in an incubator at 37°C and 5% CO_2. SH-SY5Y cells were grown and differentiated according to Presgraves, *et al* [18]. Cells were treated with 50 µM DB for 24 hours, washed three times with ice-cold PBS, and lysed cold in mRIPA buffer (50 mM Tris pH 7.8, 1 mM EDTA, 150 mM NaCl, 1% NP40, 0.25% Sodium Deoxycholate) supplemented with Halt protease inhibitor cocktail (100x, Thermo). Protein lysates were sonicated in a Cup Horn sonicator

(QSonica) for 20 minutes (30s on/off). The sonication cup must be filled with ice and replenished after 10 minutes to keep samples cold. Lysates are clarified by centrifugation at 21,000 x g and 4°C for 10 minutes. The supernatant containing the soluble protein fraction was transferred to a fresh microcentrifuge tube. The protein content was measured using Pierce 660 nm Assay Reagent (Thermo Scientific) using a BSA standard curve.

For each enrichment, 10 µL of NanoLink beads were washed two times with PBS, mixed with 500 µg of protein, and incubated with end-over-end rotation for one hour at room temperature. Beads were washed two times with mRIPA buffer, once with 1 M KCl, once with 0.1 M Na_2CO_3, and twice with 2 M Urea (50 mM Tris pH 8). Beads were resuspended in 100 µL 8 M Urea (50 mM Tris pH 8, 150 mM NaCl), reduced with 1 mM TCEP and alkylated with 2 mM CAM. Urea was diluted to under 1.5 M with 100 mM triethylammonium bicarbonate buffer. Proteins were digested off beads with 0.25 µg Lys-C for 2 hours, followed by 0.25 µg Trypsin overnight. Peptides were acidified to pH 2 with t 10% TFA and desalted on StageTips [95]. Peptides were then dried via speedvac and resuspended in StageTip Buffer A.

LC-MS/MS and data analysis

Peptides were separated on a Thermo-Dionex RSLCNano UHPLC instrument with 10 cm long fused silica capillary columns made in-house with a laser puller (Sutter) and packed with 3 µm 120 Å reversed phase C18 beads (Dr. Maisch). The LC gradient was 90 min long with 10–35% B at 200 nL/min. LC solvent A was 0.1% acetic acid and LC solvent B was 0.1% acetic acid, 99.9% acetonitrile. MS data was collected with a Thermo Orbitrap Elite spectrometer. Data-dependent analysis was applied using Top15 selection with CID fragmentation. Raw files were analyzed by MaxQuant/Andromeda [72] version 1.5.7.4 using protein, peptide and site FDRs of 0.01 and a score minimum of 40 for modified peptides, 0 for unmodified peptides; delta score minimum of 6 for modified peptides, 0 for unmodified peptides. MS/MS spectra were searched against the UniProt human database (updated July, 2016). MaxQuant search parameters: Variable modifications included Oxidation (M) and Acetyl (Protein N-term). Carbamidomethyl (C) was a fixed modification. Max. missed cleavages was 2, enzyme was Trypsin/P, max. charge was 7. The MaxQuant match between runs feature was enabled. The initial search tolerance for FTMS scans was 20 ppm and 0.5 Da for ITMS MS/MS scans. Data was further processed using the Perseus software package (version 1.5.8.5), the R environment, and Microsoft Excel. Significantly

enriched proteins in the 50 μM BD experiments were determined by applying a moderated two-tailed, two-sample *t* test in Perseus with an FDR of 0.05 and a small constant s0 = 0.1.

Immunofluorescence (IF)

HEK293 cells stably expressing VMAT2 and DAT were gifted by Dr. Gary Miller (Columbia). Cells were grown in DMEM media supplemented with 10% FBS (Hyclone, GE) and Penicillin-Streptomycin-Glutamine (100X, Thermo Scientific), 100 μg/ml Zeocin (Invitrogen) and 250 μg/ml G-418 (GoldBio) in an incubator at 37°C and 5% CO_2. For BD experiments, the same protocol was followed.

Cells were plated on acid washed cover slips and grown to 60% confluence. Fresh media was added 16-18 hours prior to DA treatment (the day before). Cells were treated with 50 μM DA for 24 hours. DA was made at 1000x stock in PBS and aliquots were frozen at -80°C. It is important to avoid freeze/thaw cycles as DA will oxidize quickly. After treatment, cells were washed 3X with ice-cold PBS and fixed with 4% paraformaldehyde for 20 minutes. Coverslips were washed three times with PBS, quenched with 50 mM NH_4Cl, washed again, and permeabilized with 0.1% TritonX-100 for four minutes at room temperature. Slips were washed again, and blocked in 2% goat serum, 1% bovine serum albumin (BSA) in PBS for one hour. After blocking, slips were washed once with PBS before incubation with primary antibody (DAT 1:200, Tom20 1:500) in 0.2% goat serum, 0.1% Tween-20, 0.5% BSA in PBS at 4°C overnight. Slips were washed three times with PBS, and secondary antibody (1:500, diluted into same buffer at primary antibody) with NucBlue and AvidinGreen (were specified) for one hour at room temperature. Slips were washed three times with PBS, once with water, and mounted with ProLong Antifade Diamond (Invitrogen) and cured overnight.

Confocal Microscopy

IF experiments were imaged on a Leica SP8X Confocal Microscope. For nIRF experiments, the following settings were used: The scan direction was unidirectional at 200 Hz. Images were taken at 63X in oil immersion. The aperture was set to 1.4, and the pinhole was calculated for 700 nM and set to 115.3 μm. Images were collective with a line average of 3 and a frame average 1. UV laser was set to 3% and detected in PMT, Alexa 488 or 555 was excited with laser at 5% power and detected in PMT. The nIRF

was excited at 670 nm with the laser power at 50% and detected in HyD. Images were processed in ImageJ.

3.4. Discussion

We describe two alternative strategies to study dopaminylation: biotin-dopamine and nIRF. A biotinylated dopamine molecule is attractive as many tools already exist to enrich or visualize biotinylation. However, we first needed to determine if BD is comparable to DA. Our data indicates that BD has similar properties to dopamine in that BD modifies cysteine residues in standard peptides and modifies proteins in cultured cells. Furthermore, the BD maintains its reactive catechol group; the two hydroxyl groups on the benzene ring are critical for BD modification as biotin-tyramide is unable to modify proteins in cultured cells. Another potential benefit of using BD is that it is applied exogenously, it crosses cell membranes and therefore BD can be used in multiple cell types. Here, we show the BD modifies proteins in both mouse neuroblastoma cells (N2A) and differentiated human neuroblatoma cells (dSH-SY5Y) without requiring expression of dopamine transporters or specialized peroxidases.

We utilized several biotin-avidin tools to study biotin-dopaminylation of proteins including affinity pull-downs coupled with LC-MS/MS. From these studies, we identified several proteins of interest in neurodegeneration including tau, gephyrin, and reticulin-3, which are found in protein plaques in human brain. Comparing our data set from BD experiments to proteins we found dopaminylated in our PBA experiments, we see a 3% overlap in our dopaminylated proteins from HEK-VMAT cells and biotin-dopaminylated proteins from N2A cells. This may be partially due to differential susceptibility to dopamine oxidation between species. Furthermore, we noticed our human cells were more vulnerable to high doses of BD or DA than mouse cells, which may be expected as mouse cells are known to be more resistant to the toxic effects of DA [64]. Comparing biotin-dopaminylated proteins from differentiated SH-SY5Y and dopaminylated proteins from HEK-VMAT cells, we found 12% of modified proteins are common between BD and DA. While some differences may be due to differential gene expression, we wanted to look for direct evidence of biotin-dopaminylation of proteins. Unfortunately, the biotin moieties are difficult to elute from solid phase streptavidin beads and attempts to identify sites of biotinylation yield

few results. We iterated through several attempts to use biotin antibodies for biotin-dopaminylation site ID [84], but were unable to successfully enrich biotin-dopaminylated peptides.

Throughout our study of BD, some differences between dopamine and biotin-dopamine were observed. For example, BD appears to be more stable in solution than DA and BD solutions color much more slowly. Also, BD does not form black pigments in a comparable time to DA. Whereas DA turns pinkish within hours at room temperature and form black pigments in a few days, BD colors only after several days and we never observed pigmentation. This may be due to the modified amine group blocking cyclization making polymerization occur through alternative pathways. A modified amine group may also slow the oxidation rate for BD. Together, these differences may have implications for BD modification in cells.

Finally, while biotin-dopamine may be an interesting tool to probe proteins of interest like tau, our biotin-dopamine approach cannot be translated to study tissue. Our method for covalent capture of dopaminylated peptides described in Chapter 2 can be used to study dopaminylation from endogenous DA modification and does not require derivatization of dopamine analogs. Biotin-dopamine may benefit from future study to identify modified residues or be used as a chemical probe in living cells, but this is beyond the scope of this work.

To get a more visual based detection approach, we tested nIRF confocal imaging for the detection of dopaminylation in cultured cells. These experiments aimed to complement our identification of dopaminylated peptides (Chapter 2) and were an extension of the work done by Mazzulli *et al.,* to detect and quantify oxidized catechols by nIRF. Confocal microscopy using nIRF to detect oxidized DA represents a potential method to track dopaminylation in fixed tissue. Our experiments with confocal microscopy and nIRF suggest fluorescence specific to DA treated cells. However, we found the signal to noise ratio to be fairly low and difficult to interpret. Unlike fluorophore-based IF, nIRF of dopaminylation relies on direct detection of the *o*-quinone and no amplification of signal is possible. Unable to increase the fluorescent signal, we are unable to determine if the nIRF signal is co-localizing with organelles or proteins of interest. Lastly, we saw background signal in our control experiments (no DA treatments) increased over time, making re-imaging of microscope slides difficult. Overall, we believe this technique

shows some promise, but needs further work and optimization to ensure a robust method to detect dopaminylation by confocal microscopy.

3.5. Supplemental Figures

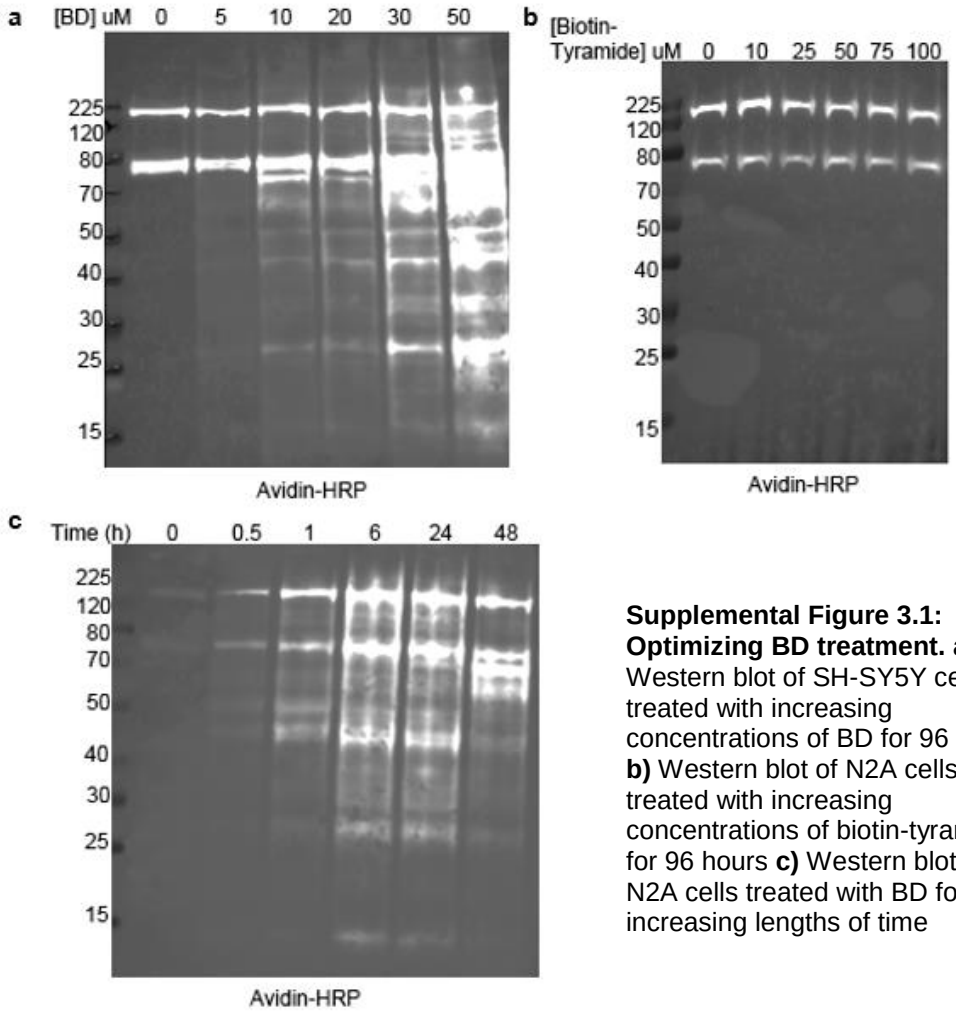

Supplemental Figure 3.1: Optimizing BD treatment. a) Western blot of SH-SY5Y cells treated with increasing concentrations of BD for 96 hours **b)** Western blot of N2A cells treated with increasing concentrations of biotin-tyramide for 96 hours **c)** Western blot of N2A cells treated with BD for increasing lengths of time

1. Schultz, W., *Behavioral dopamine signals.* Trends Neurosci, 2007. **30**(5): p. 203-10.
2. Palmiter, R.D., *Dopamine Signaling as a Neural Correlate of Consciousness.* Neuroscience, 2011. **198**: p. 213-220.
3. Medina, M.A., et al., *Biogenic amines and polyamines: Similar biochemistry for different physiological missions and biomedical applications.* Critical Reviews in Biochemistry and Molecular Biology, 2003. **38**(1): p. 23-59.
4. Canovas, F.G., et al., *The role of pH in the melanin biosynthesis pathway.* J Biol Chem, 1982. **257**(15): p. 8738-44.
5. Lohr, K.M., et al., *Membrane transporters as mediators of synaptic dopamine dynamics: implications for disease.* Eur J Neurosci, 2017. **45**(1): p. 20-33.
6. Neve, K.A., J.K. Seamans, and H. Trantham-Davidson, *Dopamine receptor signaling.* J Recept Signal Transduct Res, 2004. **24**(3): p. 165-205.
7. Marchitti, S.A., R.A. Deitrich, and V. Vasiliou, *Neurotoxicity and metabolism of the catecholamine-derived 3,4-dihydroxyphenylacetaldehyde and 3,4-dihydroxyphenylglycolaldehyde: the role of aldehyde dehydrogenase.* Pharmacol Rev, 2007. **59**(2): p. 125-50.
8. Sharman, D.F., *The catabolism of catecholamines. Recent studies.* Br Med Bull, 1973. **29**(2): p. 110-5.
9. Cobley, J.N., M.L. Fiorello, and D.M. Bailey, *13 reasons why the brain is susceptible to oxidative stress.* Redox Biology, 2018. **15**: p. 490-503.
10. Lee, H., et al., *Mussel-inspired surface chemistry for multifunctional coatings.* Science, 2007. **318**(5849): p. 426-30.
11. Jiang, L.Q., et al., *Surface ocean pH and buffer capacity: past, present and future.* Sci Rep, 2019. **9**(1): p. 18624.
12. Lee, K., et al., *Role of Dopamine Chemistry in the Formation of Mechanically Strong Mandibles of Grasshoppers.* Chemistry of Materials, 2015. **27**(19): p. 6478-6481.
13. Carlsson, A., et al., *On the presence of 3-hydroxytyramine in brain.* Science, 1958. **127**(3296): p. 471.
14. Bjorklund, A. and S.B. Dunnett, *Dopamine neuron systems in the brain: an update.* Trends Neurosci, 2007. **30**(5): p. 194-202.
15. Dichter, G.S., C.A. Damiano, and J.A. Allen, *Reward circuitry dysfunction in psychiatric and neurodevelopmental disorders and genetic syndromes: animal models and clinical findings.* J Neurodev Disord, 2012. **4**(1): p. 19.
16. Gerfen, C.R. and D.J. Surmeier, *Modulation of striatal projection systems by dopamine.* Annu Rev Neurosci, 2011. **34**: p. 441-66.
17. Grace, A.A., *Dysregulation of the dopamine system in the pathophysiology of schizophrenia and depression.* Nat Rev Neurosci, 2016. **17**(8): p. 524-32.
18. Willuhn, I., et al., *Excessive cocaine use results from decreased phasic dopamine signaling in the striatum.* Nat Neurosci, 2014. **17**(5): p. 704-9.
19. Rangel-Barajas, C., I. Coronel, and B. Floran, *Dopamine Receptors and Neurodegeneration.* Aging Dis, 2015. **6**(5): p. 349-68.
20. Jankovic, J., *Parkinson's disease: clinical features and diagnosis.* J Neurol Neurosurg Psychiatry, 2008. **79**(4): p. 368-76.
21. Postuma, R.B., et al., *Identifying prodromal Parkinson's disease: pre-motor disorders in Parkinson's disease.* Mov Disord, 2012. **27**(5): p. 617-26.

22. Kalia, L.V. and A.E. Lang, *Parkinson disease in 2015: Evolving basic, pathological and clinical concepts in PD.* Nat Rev Neurol, 2016. **12**(2): p. 65-6.
23. Verstraeten, A., J. Theuns, and C. Van Broeckhoven, *Progress in unraveling the genetic etiology of Parkinson disease in a genomic era.* Trends Genet, 2015. **31**(3): p. 140-9.
24. Spatola, M. and C. Wider, *Genetics of Parkinson's disease: the yield.* Parkinsonism Relat Disord, 2014. **20 Suppl 1**: p. S35-8.
25. Bellomo, G., et al., *The vicious cycle between alpha-synuclein aggregation and autophagic-lysosomal dysfunction.* Mov Disord, 2019.
26. Vogels, T., et al., *Propagation of Tau Pathology: Integrating Insights From Postmortem and In Vivo Studies.* Biol Psychiatry, 2019.
27. Telling, N.D., et al., *Iron Biochemistry is Correlated with Amyloid Plaque Morphology in an Established Mouse Model of Alzheimer's Disease.* Cell Chem Biol, 2017. **24**(10): p. 1205-1215 e3.
28. Wright, J.A., X. Wang, and D.R. Brown, *Unique copper-induced oligomers mediate alpha-synuclein toxicity.* FASEB J, 2009. **23**(8): p. 2384-93.
29. Wan, W., et al., *Iron Deposition Leads to Neuronal alpha-Synuclein Pathology by Inducing Autophagy Dysfunction.* Front Neurol, 2017. **8**: p. 1.
30. Bellou, V., et al., *Environmental risk factors and Parkinson's disease: An umbrella review of meta-analyses.* Parkinsonism Relat Disord, 2016. **23**: p. 1-9.
31. Goldman, S.M., et al., *Genetic modification of the association of paraquat and Parkinson's disease.* Mov Disord, 2012. **27**(13): p. 1652-8.
32. Monzani, E., et al., *Dopamine, Oxidative Stress and Protein-Quinone Modifications in Parkinson's and Other Neurodegenerative Diseases.* Angewandte Chemie-International Edition, 2019. **58**(20): p. 6512-6527.
33. Harrington, K.A., et al., *Dopamine transporter (Dat) and synaptic vesicle amine transporter (VMAT2) gene expression in the substantia nigra of control and Parkinson's disease.* Brain Res Mol Brain Res, 1996. **36**(1): p. 157-62.
34. Pifl, C., et al., *Is Parkinson's disease a vesicular dopamine storage disorder? Evidence from a study in isolated synaptic vesicles of human and nonhuman primate striatum.* J Neurosci, 2014. **34**(24): p. 8210-8.
35. Lohr, K.M., et al., *Increased vesicular monoamine transporter enhances dopamine release and opposes Parkinson disease-related neurodegeneration in vivo.* Proc Natl Acad Sci U S A, 2014. **111**(27): p. 9977-82.
36. Rilstone, J.J., R.A. Alkhater, and B.A. Minassian, *Brain dopamine-serotonin vesicular transport disease and its treatment.* N Engl J Med, 2013. **368**(6): p. 543-50.
37. Jellinger, K., et al., *Chemical evidence for 6-hydroxydopamine to be an endogenous toxic factor in the pathogenesis of Parkinson's disease.* J Neural Transm Suppl, 1995. **46**: p. 297-314.
38. Galzigna, L., A. De Iuliis, and L. Zanatta, *Enzymatic dopamine peroxidation in substantia nigra of human brain.* Clin Chim Acta, 2000. **300**(1-2): p. 131-8.
39. Hastings, T.G., *Enzymatic oxidation of dopamine: the role of prostaglandin H synthase.* J Neurochem, 1995. **64**(2): p. 919-24.
40. Block, M.L., L. Zecca, and J.S. Hong, *Microglia-mediated neurotoxicity: uncovering the molecular mechanisms.* Nat Rev Neurosci, 2007. **8**(1): p. 57-69.
41. Bulk, M., et al., *Quantitative comparison of different iron forms in the temporal cortex of Alzheimer patients and control subjects.* Scientific Reports, 2018. **8**.
42. Castellani, R.J., et al., *Sequestration of iron by Lewy bodies in Parkinson's disease.* Acta Neuropathologica, 2000. **100**(2): p. 111-114.
43. Mor, D.E., et al., *Dopamine induces soluble alpha-synuclein oligomers and nigrostriatal degeneration.* Nat Neurosci, 2017. **20**(11): p. 1560-+.

44. Fedorow, H., et al., *Neuromelanin in human dopamine neurons: Comparison with peripheral melanins and relevance to Parkinson's disease.* Progress in Neurobiology, 2005. **75**(2): p. 109-124.
45. Solomon, E.I., et al., *Copper Active Sites in Biology.* Chemical Reviews, 2014. **114**(7): p. 3659-3853.
46. Zucca, F.A., et al., *Interactions of iron, dopamine and neuromelanin pathways in brain aging and Parkinson's disease.* Progress in Neurobiology, 2017. **155**: p. 96-119.
47. Zucca, F.A., et al., *Neuromelanin organelles are specialized autolysosomes that accumulate undegraded proteins and lipids in aging human brain and are likely involved in Parkinson's disease.* Npj Parkinsons Disease, 2018. **4**.
48. Shima, T., et al., *Binding of iron to neuromelanin of human substantia nigra and synthetic melanin: An electron paramagnetic resonance spectroscopy study.* Free Radical Biology and Medicine, 1997. **23**(1): p. 110-119.
49. Sulzer, D., et al., *Neuronal pigmented autophagic vacuoles: lipofuscin, neuromelanin, and ceroid as macroautophagic responses during aging and disease.* J Neurochem, 2008. **106**(1): p. 24-36.
50. Marsden, C.D., *Pigmentation in the nucleus substantiae nigrae of mammals.* J Anat, 1961. **95**: p. 256-61.
51. Marsden, C.D., *The Development of Pigmentation and Enzyme Activity in the Nucleus Substantiae Nigrae of the Cat.* J Anat, 1965. **99**: p. 175-80.
52. Zecca, L., et al., *The absolute concentration of nigral neuromelanin, assayed by a new sensitive method, increases throughout the life and is dramatically decreased in Parkinson's disease.* Febs Letters, 2002. **510**(3): p. 216-220.
53. Venkateshappa, C., et al., *Increased oxidative damage and decreased antioxidant function in aging human substantia nigra compared to striatum: Implications for Parkinson's disease.* Movement Disorders, 2014. **29**: p. S35-S35.
54. Tribl, F., et al., *Identification of L-ferritin in neuromelanin granules of the human substantia nigra: a targeted proteomics approach.* Mol Cell Proteomics, 2009. **8**(8): p. 1832-8.
55. D'Amato, R.J., Z.P. Lipman, and S.H. Snyder, *Selectivity of the parkinsonian neurotoxin MPTP: toxic metabolite MPP+ binds to neuromelanin.* Science, 1986. **231**(4741): p. 987-9.
56. Lindquist, N.G., B.S. Larsson, and A. Lyden-Sokolowski, *Autoradiography of [14C]paraquat or [14C]diquat in frogs and mice: accumulation in neuromelanin.* Neurosci Lett, 1988. **93**(1): p. 1-6.
57. Haining, R.L. and C. Achat-Mendes, *Neuromelanin, one of the most overlooked molecules in modern medicine, is not a spectator.* Neural Regen Res, 2017. **12**(3): p. 372-375.
58. Zucca, F.A., et al., *Neuromelanin of the human substantia nigra: an update.* Neurotox Res, 2014. **25**(1): p. 13-23.
59. Viceconte, N., et al., *Neuromelanin activates proinflammatory microglia through a caspase-8-dependent mechanism.* J Neuroinflammation, 2015. **12**: p. 5.
60. Li, H. and G. Dryhurst, *Irreversible inhibition of mitochondrial complex I by 7-(2-aminoethyl)-3,4-dihydro-5-hydroxy-2H-1,4-benzothiazine-3-carboxyli c acid (DHBT-1): a putative nigral endotoxin of relevance to Parkinson's disease.* J Neurochem, 1997. **69**(4): p. 1530-41.
61. Ito, S., A. Palumbo, and G. Prota, *Tyrosinase-catalyzed conjugation of dopa with glutathione.* Experientia, 1985. **41**(7): p. 960-1.
62. Xu, R., et al., *Characterization of products from the reactions of N-acetyldopamine quinone with N-acetylhistidine.* Arch Biochem Biophys, 1996. **329**(1): p. 56-64.
63. Van Laar, V.S., et al., *Proteomic identification of dopamine-conjugated proteins from isolated rat brain mitochondria and SH-SY5Y cells.* Neurobiol Dis, 2009. **34**(3): p. 487-500.
64. Burbulla, L.F., et al., *Dopamine oxidation mediates mitochondrial and lysosomal dysfunction in Parkinson's disease.* Science, 2017. **357**(6357): p. 1255-1261.

65. Belluzzi, E., et al., *Human SOD2 modification by dopamine quinones affects enzymatic activity by promoting its aggregation: possible implications for Parkinson's disease.* PLoS One, 2012. **7**(6): p. e38026.
66. Mexas, L.M., V.R. Florang, and J.A. Doorn, *Inhibition and covalent modification of tyrosine hydroxylase by 3,4-dihydroxyphenylacetaldehyde, a toxic dopamine metabolite.* Neurotoxicology, 2011. **32**(4): p. 471-7.
67. Werner-Allen, J.W., et al., *Toxic Dopamine Metabolite DOPAL Forms an Unexpected Dicatechol Pyrrole Adduct with Lysines of alpha-Synuclein.* Angew Chem Int Ed Engl, 2016. **55**(26): p. 7374-8.
68. Longhena, F., et al., *The Contribution of alpha-Synuclein Spreading to Parkinson's Disease Synaptopathy.* Neural Plast, 2017. **2017**: p. 5012129.
69. Kalousova, M., J. Skrha, and T. Zima, *Advanced glycation end-products and advanced oxidation protein products in patients with diabetes mellitus.* Physiol Res, 2002. **51**(6): p. 597-604.
70. van der Mijn, J.C., et al., *Evaluation of different phospho-tyrosine antibodies for label-free phosphoproteomics.* J Proteomics, 2015. **127**(Pt B): p. 259-63.
71. Herberg, S., et al., *Histone H3 lysine 9 trimethylation is required for suppressing the expression of an embryonically activated retrotransposon in Xenopus laevis.* Sci Rep, 2015. **5**: p. 14236.
72. Cox, J., et al., *Andromeda: a peptide search engine integrated into the MaxQuant environment.* J Proteome Res, 2011. **10**(4): p. 1794-805.
73. Dietrich, J.B., et al., *Acute or repeated cocaine administration generates reactive oxygen species and induces antioxidant enzyme activity in dopaminergic rat brain structures.* Neuropharmacology, 2005. **48**(7): p. 965-74.
74. LaVoie, M.J. and T.G. Hastings, *Dopamine quinone formation and protein modification associated with the striatal neurotoxicity of methamphetamine: evidence against a role for extracellular dopamine.* J Neurosci, 1999. **19**(4): p. 1484-91.
75. Granado, N., et al., *Persistent MDMA-induced dopaminergic neurotoxicity in the striatum and substantia nigra of mice.* J Neurochem, 2008. **107**(4): p. 1102-12.
76. Lotharius, J. and K.L. O'Malley, *The parkinsonism-inducing drug 1-methyl-4-phenylpyridinium triggers intracellular dopamine oxidation. A novel mechanism of toxicity.* J Biol Chem, 2000. **275**(49): p. 38581-8.
77. Betarbet, R., et al., *Chronic systemic pesticide exposure reproduces features of Parkinson's disease.* Nat Neurosci, 2000. **3**(12): p. 1301-6.
78. LaVoie, M.J., et al., *Dopamine covalently modifies and functionally inactivates parkin.* Nat Med, 2005. **11**(11): p. 1214-21.
79. Malaker, S.A., et al., *Identification of Glycopeptides as Posttranslationally Modified Neoantigens in Leukemia.* Cancer Immunol Res, 2017. **5**(5): p. 376-384.
80. Zhang, Y., et al., *Site-specific characterization of the Asp- and Glu-ADP-ribosylated proteome.* Nat Methods, 2013. **10**(10): p. 981-4.
81. Burzio, L.A. and J.H. Waite, *Cross-linking in adhesive quinoproteins: studies with model decapeptides.* Biochemistry, 2000. **39**(36): p. 11147-53.
82. Mazzulli, J.R., et al., *Detection of Free and Protein-Bound ortho-Quinones by Near-Infrared Fluorescence.* Anal Chem, 2016. **88**(4): p. 2399-405.
83. Napolitano, A., P. Manini, and M. d'Ischia, *Oxidation chemistry of catecholamines and neuronal degeneration: an update.* Curr Med Chem, 2011. **18**(12): p. 1832-45.
84. Udeshi, N.D., et al., *Antibodies to biotin enable large-scale detection of biotinylation sites on proteins.* Nat Methods, 2017. **14**(12): p. 1167-1170.
85. Presgraves, S.P., et al., *Terminally differentiated SH-SY5Y cells provide a model system for studying neuroprotective effects of dopamine agonists.* Neurotox Res, 2004. **5**(8): p. 579-98.

86. Bernstein, A.I., K.A. Stout, and G.W. Miller, *A fluorescent-based assay for live cell, spatially resolved assessment of vesicular monoamine transporter 2-mediated neurotransmitter transport.* J Neurosci Methods, 2012. **209**(2): p. 357-66.
87. Geiger, T., et al., *Comparative proteomic analysis of eleven common cell lines reveals ubiquitous but varying expression of most proteins.* Mol Cell Proteomics, 2012. **11**(3): p. M111 014050.
88. Smith, D.G., R. Cappai, and K.J. Barnham, *The redox chemistry of the Alzheimer's disease amyloid beta peptide.* Biochim Biophys Acta, 2007. **1768**(8): p. 1976-90.
89. Abo, M. and E. Weerapana, *A Caged Electrophilic Probe for Global Analysis of Cysteine Reactivity in Living Cells.* J Am Chem Soc, 2015. **137**(22): p. 7087-90.
90. Barretina, J., et al., *The Cancer Cell Line Encyclopedia enables predictive modelling of anticancer drug sensitivity.* Nature, 2012. **483**(7391): p. 603-7.
91. Hedges, D.M., et al., *Methamphetamine Induces Dopamine Release in the Nucleus Accumbens Through a Sigma Receptor-Mediated Pathway.* Neuropsychopharmacology, 2018. **43**(6): p. 1405-1414.
92. Park, S.U., et al., *Peroxynitrite inactivates the human dopamine transporter by modification of cysteine 342: potential mechanism of neurotoxicity in dopamine neurons.* J Neurosci, 2002. **22**(11): p. 4399-405.
93. Rastedt, D.E., R.A. Vaughan, and J.D. Foster, *Palmitoylation mechanisms in dopamine transporter regulation.* J Chem Neuroanat, 2017. **83-84**: p. 3-9.
94. Alvarez-Zaldiernas, C., et al., *Cellular Redox Systems Impact the Aggregation of Cu,Zn Superoxide Dismutase Linked to Familial Amyotrophic Lateral Sclerosis.* J Biol Chem, 2016. **291**(33): p. 17197-208.
95. Rappsilber, J., M. Mann, and Y. Ishihama, *Protocol for micro-purification, enrichment, pre-fractionation and storage of peptides for proteomics using StageTips.* Nat Protoc, 2007. **2**(8): p. 1896-906.
96. Rikova, K., et al., *Global survey of phosphotyrosine signaling identifies oncogenic kinases in lung cancer.* Cell, 2007. **131**(6): p. 1190-203.
97. Rhee, H.W., et al., *Proteomic mapping of mitochondria in living cells via spatially restricted enzymatic tagging.* Science, 2013. **339**(6125): p. 1328-1331.
98. Mick, D.U., et al., *Proteomics of Primary Cilia by Proximity Labeling.* Dev Cell, 2015. **35**(4): p. 497-512.
99. Myers, S.A., et al., *Discovery of proteins associated with a predefined genomic locus via dCas9-APEX-mediated proximity labeling.* Nat Methods, 2018. **15**(6): p. 437-439.
100. Goedert, M., D.S. Eisenberg, and R.A. Crowther, *Propagation of Tau Aggregates and Neurodegeneration.* Annu Rev Neurosci, 2017. **40**: p. 189-210.
101. Hales, C.M., et al., *Abnormal gephyrin immunoreactivity associated with Alzheimer disease pathologic changes.* J Neuropathol Exp Neurol, 2013. **72**(11): p. 1009-15.
102. Heath, J.E., et al., *Widespread distribution of reticulon-3 in various neurodegenerative diseases.* Neuropathology, 2010. **30**(6): p. 574-9.
103. Attems, J. and K. Jellinger, *Proteomics for synaptic markers of cognitive decline in neurodegenerative diseases.* Brain, 2018. **141**(2): p. 329-331.
104. Chen, Y.F., et al., *Cisd2 deficiency drives premature aging and causes mitochondria-mediated defects in mice.* Genes Dev, 2009. **23**(10): p. 1183-94.
105. Sanchez-Ortiz, E., et al., *Protein phosphatase 5 protects neurons against amyloid-beta toxicity.* J Neurochem, 2009. **111**(2): p. 391-402.
106. Ayuso, P., et al., *A polymorphism located at an ATG transcription start site of the heme oxygenase-2 gene is associated with classical Parkinson's disease.* Pharmacogenet Genomics, 2011. **21**(9): p. 565-71.

107. Sturner, E. and C. Behl, *The Role of the Multifunctional BAG3 Protein in Cellular Protein Quality Control and in Disease.* Front Mol Neurosci, 2017. **10**: p. 177.
108. Riquier, S., et al., *Peroxiredoxin post-translational modifications by redox messengers.* Redox Biology, 2014. **2**: p. 777-85.
109. Wu, C., et al., *Sulfonation of the resolving cysteine in human peroxiredoxin 1: A comprehensive analysis by mass spectrometry.* Free Radic Biol Med, 2017. **108**: p. 785-792.
110. Ikwegbue, P.C., et al., *Roles of Heat Shock Proteins in Apoptosis, Oxidative Stress, Human Inflammatory Diseases, and Cancer.* Pharmaceuticals (Basel), 2017. **11**(1).
111. Castegna, A., et al., *Proteomic identification of oxidatively modified proteins in Alzheimer's disease brain. Part II: dihydropyrimidinase-related protein 2, alpha-enolase and heat shock cognate 71.* J Neurochem, 2002. **82**(6): p. 1524-32.

Vita

Emily Jane Myers was born in Fullerton, California. After graduating high school, she attended Fullerton Community College prior to transferring to the University of California, Irvine. Emily earned a Bachelor of Science from the University of California Irvine in Biochemistry and Molecular Biology in 2011. While working on her undergraduate degree, Emily worked in the lab of Dr. Jefferson Y Chan where she investigated Nrf1 trafficking via retrotranslocation of deglycosylated substrates and validation of novel genes under Nrf1 transcriptional control in disease state and cell lines. After graduation, Emily worked as a project coordinator and researcher for the Women's Interagency HIV Study at the University of Southern California investigating accelerating aging mechanisms due to latent HIV infection. In 2013, she joined the University of Washington's Department of Pharmacology as a graduate research associate, and earned a Doctor of Philosophy in 2019.